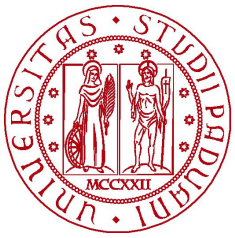

UNIVERSITÀ DEGLI STUDI DI PADOVA

UNIVERSITÁ DEGLI STUDI DI PADOVA

Dipartimento di Ingegneria Idraulica, Marittima, Ambientale e Geotecnica

Scuola di Dottorato di Ricerca in

Scienze dell'Ingegneria Civile e Ambientale

XXIV Ciclo

CONTRIBUTIONS TO LONG-TERM MORPHODYNAMIC MODELLING OF ESTUARIES, LAGOONS, AND LITTORAL ZONES

Direttore della Scuola: Ch.mo Prof. Stefano Lanzoni

Supervisore: Ch.mo Prof. Giampaolo Di Silvio

Dottorando: Davide Bonaldo

A mia madre

Acknowledgements

This thesis has been made possible thanks to the helpful contributions of many people.
My deep gratitude goes to my supervisor, Prof. Giampaolo Di Silvio, for having introduced me into the Hydraulic studies and supported me with his knowledge and his patient assistance throughout all the years spent together.
I would also thank Prof. Ian Townend who gave me the opportunity to carry out my research at HR Wallingford Ltd.: our frequent and fruitful discussions provided a great improvement in the quality of my work.
I wish to acknowledge the Director of the Doctoral School, Prof. Stefano Lanzoni, all the teachers of the School, my colleagues, and all the people who supported and shared my efforts, both materially and morally.
I also wish to warmly thank my high school teachers of Literature and Philosophy, Prof. Maria Rosa Giacon and Prof. Antonio Beninati, whose teachings always remind me the importance of being human, above all.
Infine, ma *in primis*, un ringraziamento e un abbraccio alla mia famiglia, il cui affetto e sostegno incondizionati mi hanno sempre accompagnato. Grazie di cuore.

Contents

List of Tables

List of Figures

Abstract

In the present thesis I will resume the formulation and some applications of a two-dimensional mathematical model for the long-term representation of the morphodynamic processes which take place in tidal environments. I will refer to non-cohesive sediments, eventually with non uniform grain size.

In the conceptualization presented here the large-scale morphodynamic problem is described based on the concepts of *Transport Concentration* and *Intertidal Dispersion*, directly resulting from an appropriate time averaging operation and from an empirical approach to the uncertainties of the problem.

The results of the research activity will be presented in four chapters, each one is meant to enclose completely a conceptual unit of the work performed; these units are preceded by a general outline in which various aspects of the problem are synthesized and contextualised. First the theoretical fundamentals of the model and its multigranular extension will be presented, highlighting the role of the main exogenous forcing factors (tidal range, wind, subsidence and sea level rise) in defining morphology and grain size distribution of tidal environments. Then two applications of the model will be illustrated: the first one studies the impact of different anthropic interventions on a tidal lagoon, the second one aims to quantify the morphodynamic effect of the nodal perturbation of the tidal amplitude.

The thesis is concluded by some considerations on the validity limitations of the model as currently formulated and with some proposals aimed to extending its applicability

to complex systems in which the fluvial, estuarine and coastal environment mutually interact at the historical and geological temporal and spatial scales.

Sommario

Nel presente lavoro si espongono la formulazione ed alcune applicazioni di un modello matematico bidimensionale per la rappresentazione a lungo termine dei processi morfodinamici che interessano un ambiente a marea, in presenza di sedimenti non coesivi eventualmente a granulometria non uniforme.

Nella concettualizzazione qui presentata il problema morfodinamico a grande scala spaziale viene descritto sulla base dei concetti di *Concentrazione di Trasporto* e *Dispersione Intermareale*, derivanti direttamente da una opportuna operazione di media temporale e da un approccio empirico alla gestione delle incertezze del problema.

I risultati dell'attività di ricerca saranno presentati in quattro capitoli, ciascuno dei quali è inteso a racchiudere compiutamente un nucleo concettuale del lavoro svolto, preceduti da un inquadramento generale in cui i vari aspetti del problema sono sintetizzati e contestualizzati. Dapprima si presenteranno i fondamenti teorici del modello e la sua estensione multigranulare, evidenziando il ruolo delle principali forzanti esogene (ampiezza di marea, vento, subsidenza e innalzamento del livello del mare) nel definire morfologia e granulometria degli ambienti a marea. Quindi si illustreranno due applicazioni del modello: la prima volta a studiare l'impatto esercitato da vari interventi antropici su una laguna a marea, la seconda finalizzata a quantificare l'effetto morfodinamico della perturbazione nodale dell'ampiezza di marea.

La trattazione si conclude con alcune considerazioni sui limiti di validità del modello così come formulato allo stato attuale, e con alcune proposte volte ad estenderne

l'applicabilità a sistemi complessi, nei quali gli ambienti fluviale, estuarino e costiero interagiscono mutuamente alle scale spaziali e temporali che sono proprie dei processi storici e geologici.

Chapter 1

Introduction

1.1 Overview

Long-term morphodynamic modelling is a fundamental tool in understanding and managing coastal and estuarine environments. Due to the complexity of the phenomena, the great amount of uncertainties, and the unaffordable computational requirement of a full-detailed representation, some simplifications are required. In this document we present the main points of the formulation and improvement of a long-term, two dimensional morphodynamic model for tidal systems, and some applications. The research work carried out during my Ph.D. course is reported with some detail in four papers, one published and three submitted, each one focusing on the main conceptual units of the work and costituting the subject for each Chapter of the present thesis.

The first Chapter introduces the basic concepts of the *Intertidal Model* with reference to unigranular sediments and shows the effects of some forcing factors on the overall morphological configuration of a tidal lagoon. The second one extends the model to the case of graded sediments with non cohesive behaviour, and investigates the mechanisms controlling spatial segregation of sediments within a basin. In doing that, a deeper insight on the conceptualization of some resuspension factors such as tidal currents and

sea waves is provided. Furthermore, a schematic representation of the interface between the sea and the lagoon (a sort of *inlet submodel*) is presented. This submodel can be used for defining the external boundary conditions of the lagoon with no need for an explicit representation of littoral area.

In the third Chapter the Multigranular Intertidal Model is applied to the case of a schematic lagoon comparable, for dimensions and configuration, to the Central Basin of the lagoon of Venice. The effects of documented human interventions over four centuries of history are investigated.

The fourth Chapter presents the morphological effect of the nodal modulation of the tidal range on a tidal lagoon.

The present thesis is concluded by a Chapter in which some topics related to the main theme of the thesis and already preliminarly investigated are discussed for their eventual developments.

1.2 Long-term model of planimetric and bathymetric evolution of a tidal lagoon

Throughout all the research work presented in this thesis, morphodynamic processes have been described as the result of the long-term transport phenomena involving the *Time-Averaged Concentration* (also called *Transport Concentration*) of sediments. Bathimetric changes in the bottom are represented as the sum of subsidence, sea level rise, and net erosion: the latter is proportional to the difference between the Transport Concentration and the *Equilibrium Concentration*, defined as the concentration giving rise, for the local hydrodynamic conditions, to nil vertical fluxes.

The equilibrium concentration accounts for water currents, sea waves and internal wind waves, and can be computed as a function of local depth by a proper manipulation of a monomial transport formula. For each resuspension factor, all the uncertainties are

lumped in a *stirring coefficient* which needs to be empirically calibrated. This formulation allows on one hand to easily treat the equilibrium concentration as an additive quantity, and on the other hand to investigate the relative effect of each stirring factor in the different morphological features. In particular, the exponent of the bottom depth in the different contributions to the Equilibrium Concentration shows that, while the effect of wind waves dominates on the shoals, tidal currents are the main resuspension factor on the channels. Where some topographical requirements are fulfilled the growth of a vegetation cover is represented and the Equilibrium Concentration is drastically lowered (eventually set to zero), in order to represent the sediment trapping and bottom strengthening due to the presence of alophile vegetation.

Sediment transport is represented, at the long time scale, as a *Tidal Dispersion* resulting from the time-integrated effect of an appropriate number of tidal cycles, plus eventually a convective effect due to the residual term rising for example from the presence of non negligible eulerian currents. The Tidal Dispersion effect is controlled by a tensor whose components are proportional to the square power of the velocity components in reference hydrodynamic conditions.

The flow field, necessary for the quantification of the tidal currents contribution to the equilibrium concentration and of the tidal dispersion components, is calculated with reference to the maximum flood conditions by a simplifed numerical sub-model. This solves the 2-D Shallow Water Equations under the hypotheses of instantaneous propagation of the tidal wave throughout a short basin and inertial terms negligible compared to the frictional ones.

The concentration flow field is computed via a Finite Element discretization of a 2-D dispersion-convection-reaction equation coming from a sediment budget within an elementary water column, and its comparison with the Equilibrium Concentration provides the bathymetric evolution in each node of the domain.

Preliminary results show here that the planimetric development of a channel network is

rather fast compared to the overall bathymetric evolution, and that its pattern is influenced by the effect of wind waves.

1.3 Morphodynamic modelling of a tidal basin in presence of graded sediments

Although several important morphodynamic processes can be reproduced by simply considering sediments with uniform composition, there are some situations in which distinguishing different sediment classes can be crucial. This is the case, for instance, of systems in which strong differences in the composition of sediments coming from different sources impede a phisically meaningful definition of the equivalent grain size; or when one wants to explain the spatial segregation of sediments throughout the basin or to perform a more accurate sediment budget within a tidal system.

For this reason, the Intertidal Model was extended into a multigranular formulation which can deal with any number of coexisting sediment classes with non cohesive behaviour. The transport mechanisms are the same listed in 1.2, but the vertical fluxes must be corrected by taking into account the grainsize composition of the bottom, which is now a further unknown in the problem. Besides the horizontal transport equation, which is the same for each sediment class except for the reaction and source terms (sediment deposition and erosion respectively), a sediment budget within the mixing layer of the bottom is now needed for closing the problem.

In absence of net fluxes the equilibrium bottom depth and composition can be analitically described as a simple function of the boundary conditions, given the channel network geometry; otherways it can be numerically attained through a reasonably long simulation. The genesis and attainment of an equilibrium configuration has been reproduced under different combinations of riverine sediment supply and subsidence and eustatism rates, in order to understand the effect of these factors on the bathimetric and

granulometric configuration of the basin. Note that, being the fluvial currents negligible in terms of transport compared to the tidal ones, the assumption of a purely dispersive system has been made.

It has thus been found that granular sediment differentiation in a tidal basin is generally related to the presence of a net horizontal flux in which a progressive sedimentation of finer matter occurs. A further, though secondary, segregation mechanism is the trapping effect acted by alophile vegetation on the salt marshes: in fact, while in absence of vegetation the bottom composition is controlled by both actual and equilibrium concentration, in presence of a completely developed vegetation cover it is only controlled by actual suspended concentration and vertical deposition rate.

It has also been shown that, even in simple conditions (only one sediment source, no net horizontal fluxes), a unigranular representation of the behaviour of a significantly graded sediment mixture can lead to somewhat misleading results. More precisely, the resulting bottom equilibrium depth tends to be overestimated, mainly due to the lack of the armouring effect acted by the coarser fraction.

In this work some attention has also been devoted on the calibration of the stirring coefficients for sea waves and tidal currents. This has been performed by using bottom and suspended sediments composition data recorded at the Lido inlet (Venice lagoon) and in the North-Eastern Adriatic littoral. Further considerations led to the definition of the boundary conditions for a tidal system, based on the calculation of the equilibrium concentration of the highest isobath, along the inlet axis, of the undisturbed littoral in the vicinity of the inlet. This operation is conceptually necessary if one wants to quantify the influence of the sea on the inner basin without requiring the complete description of the complex sediment dynamics taking place on the littoral.

It is also worth to point out that the formulation proposed in this work allows to define sediment classes based not only on their grainsize, but also on their origin. In this way the relative contributions of sea and riverine sediment supply can be evaluated in the

genesis and evolution of a tidal systems and of its sections.

1.4 Historical evolution of a micro-tidal lagoon simulated by a 2-D schematic model

The Multigranular Intertidal Model has then been used for representing the impact of human interventions on a tidal basin, by comparing different scenarios qualitatively reproducing the main events that underwent in the Venice Lagoon in the last 400 years. As first, an equilibrium condition was reached for a tidal lagoon under the joint effect of sediment input from the sea, riverine inputs, subsidence and sea level rise. In this way it was obtained a situation comparable to what the central basin of the Venice lagoon reasonably must have looked like in 1600 a.D., when the diversion of the river Brenta was completed. Starting from this configuration, four parallel evolutions have been simulated with or without the introduction of the following interventions:

1. River Brenta diversion from the Malamocco basin (≈1600 a.D.);
2. Jetties construction at the Malamocco inlet (≈1850 a.D.);
3. Increase of local subsidence due to excessive groundwater extraction (≈1950 to 1970 a.D.);
4. Excavation and maintenance of the Malamocco-Marghera navigation canal (≈1965 to nowadays).

It has been found that the river diversion, although resulting in a slow transition of the lagoon to a configuration with deeper shoals and smaller vegetated areas (and a modification of the bottom composition), seems likely to have had a lesser role in the lagoon degradation compared to the interventions acted during the last two centuries.

The construction of the jetties was represented by narrowing the inlet cross-section and modifying the boundary conditions at the sea according to the criterion mentioned in Sec. 1.3, resulting in a finer and less concentrated suspended sediment mixture. This modification produced a sudden deepening of the inlet bottom as a response to the width reduction, and then a gradual, but relevant, increase in basin erosion. Moreover, the change in composition of the boundary concentration reflects on a significant and continuous fining of the basin bottom.

The relevant anthropogenic increase in the subsidence rate, even if limited to two decades, had some effect on the whole system but particularly proved to be critical for the salt marshes, which are very sensitive to this factor and as a response to its increase lost a significant fraction of their total surface.

Dramatic effects were recorded as a consequence of the excavation and periodical dredging of the artificial channel, which acts as a trap for the sediments that come from the sea and the neighbouring shoals and that are eventually removed from the system during the dredging operations.

Although referred to an idealized situation, these results are in qualitative agreement with several evidences observed and documented for the Venice lagoon, suggesting that the model is able to capture the main processes taking place in a tidal system over hystorical period.

1.5 Morphological consequences of the nodal modulation on a tidal lagoon

The nodal modulation of the tidal range is a perturbation due to the changes in lunar declination taking place with a period of 18.6 years, and with an amplitude of the order of 4% the mean tidal range, slightly variable in time and space depending on sea level rise and local equilibrium conditions. Despite its relatively small amplitude, several Au-

thors remarked its relevance from the environmental and morphodynamic point of view. Hence the interest arose in applicating the model in the study of the morphological response of a lagoon to such a constraint, at both the *sub-nodal* and *inter-nodal* time scale. In this case, in order to reduce the complexity of the system and to easen the interpretation of the results, the unigranular formulation of the model has been applied to a schematic domain in absence of rivers and under different conditions. Simulations were performed starting from a generic non-equilibrium configuration as well as from long-term equilibrium conditions, with and without taking into account for the nodal component, and the results were post-processed via a Fourier Analysis in order to identify and compare the key features of the oscillating quantities.

It has been shown that, for a long-term time-averaged analysis (namely, at centennal or inter-nodal time scale), taking into account the nodal modulation has negligible influence on the results. On the other hand, considering the problem at a smaller time scale one finds that significant relative oscillations (eventually greater than 4%) in water depth can take place throughout the domain, particularly on the shoals. While the response of the channel network is rather prompt and synchronous, the signal propagates through the shoals in a more etherogeneous way: the results then highlight the presence of relevant oscillating fluxes not only between the system and the sea, but also among different sections of the basin itself.

Similar evidences have been obtained for different conditions of geometry, sea level rise and wind waves, showing a recurrent behaviour.

1.6 Related topics and future developments

In the previous Sections the main stages of the development and improvement of a long-term morphodinamic model for tidal systems have been summarized. Such a model can find different applications: from an engineering point of view, it can be used for exam-

ple to describe the evolutionary trend of a tidal environment or to predict the effects on landscape of different management policies.

The works presented so far focus on tidal systems in which the sea is considered as an external forcing, and some efforts have been endeavoured in understanding how does the neighbouring littoral plays its action on the system. But to a greater scale, tidal environments such as estuaries and lagoons can be seen as a component of a more complex entity involving also the littoral and the mainland in sedimentary processes at historical and geological scale. In this direction, some investigations have been carried out in long-term simplified fluvial morphodynamic modelling (published in some Conference Proceedings) and in the development of a conceptual representation of the coastal system in which fluvial, transitional and coastal environments can be treated as a whole.

Concerning the first point, some new features were introduced in an existing morphodynamic model. A simple sub-model, which can prove particularly helpful in unsurveyed rivers, was formulated providing an estimate of the hydraulic geometry of a river cross-section as a function of local slope and hydrologic regime. Furthermore, a simplified conceptualization of the interactions between river vegetation, morphology and hydrodynamics was outlined: preliminary results in this direction are rather satisfactory but a far greater dataset would be necessary to this aim.

On the littoral domain, the new element currently under formulation is the introduction, in the Intertidal Model, of a *Pseudo-Convective* term in the transport equation. Such term should represent all the processes that result in a long-term trasport of sediment but are not related to a net flux of water or to a concentration gradient. This can be the case, for example, of cross-shore transport considered at the inter-seasonal time scale; some attempts in this direction gave encouraging results.

Such a new element, eventually with the addition of a slightly more detailed description of sea waves propagation, would allow to describe the genesis of coastal formations such as spits, littoral islands, and therefore of complex transitional systems. Moreover,

it would make possible the description of sediment transport at regional scale, with applications from shore protection planning to sediment management at basin scale.

Chapter 2

Long term model of planimetric and bathymetric evolution of a tidal lagoon

2.1 Introduction

Morphological processes in tidal lagoons are controlled by tides, waves and fluvial currents and develop at different space- and time- scales. At the tidal scale (hours), sediments in suspension move from the sea into the lagoon during the flood phase and from the lagoon towards the sea during the ebb phase. At a seasonal scale (weeks) net sediment fluxes are mainly controlled by the wave climate inside and outside the lagoon. When waves produced by local winds inside the lagoon are persistent, stirred sediments leave the lagoon in larger quantities during the ebb phase; contrastingly, if there is a long period of rough sea, the quantity of sediments entering the lagoon is larger during the flood. At historical scales (decades or centuries), however, the fluxes of sediments leaving and entering the lagoon, including the positive sediment input by the rivers, tend to compensate each other. If the combined effect of eustatism (rising of the mean sea level) and subsidence (lowering of the basin bottom) is also taken into account and if the balance is perfectly closed the lagoon temporarily maintains a steady-state configu-

ration, otherwise it keeps evolving at geological or even at historical time scales.
From the ancient maps of the Lagoon of Venice it appears that the planimetric configuration of the tidal channels network remained basically the same during several centuries. Such a planimetric stability at historical scale can also be found in other lagoonal and estuarine environments. The bathymetry of the Lagoon of Venice, by contrast, is subject (since the ancient diversion of the rivers flowing into the lagoon and, even more rapidly, since the new constructions of the last 100-150 years) to a perceptible progressive evolution (Sarretta et al., 2010). Namely the depth of shoals increases, the channels tend to be silted while the tidal marshes (covered by alophile vegetation) reduce their surface area, with a net flux of sediments from marshes to shoals, from shoals to channels and eventually through the inlets out to the sea (Sarretta et al., 2010).
The morphological evolution of tidal lagoons and other coastal systems is usually investigated by short-term models (at tidal and storm time-scales), whose results are somehow combined and extrapolated to long periods. In order to study the long-term morphodynamics of lagoons and their possible steady-state configurations, however specific morphological models may also be developed, capable to account for all the different driving forces, either natural and anthropogenic. A very useful tool which has been applied to the recent evolution of the lagoon of Venice (Di Silvio, 1989) is the concept of *transport concentration* and *net sediment transport*. Since transport concentration is defined as a tidally time-averaged concentration, in some papers it has also been called *intertidal concentration*. Due to the general usage of *intertidal* to denote the elevations comprised between the tidal range, in the present chapter it has been preferred the wording *transport concentration* for expressing the tidally time-averaged concentration.
Morphological models based on this concept are very flexible and can be applied in principle with different degrees of spatial resolution (two-dimensional, one-dimensional and zero-dimensional approaches). Moreover they can incorporate a variety of complex processes such as grain size sorting, effects of vegetation, collapse of steep banks and

compaction of sediment deposits (Di Silvio and Teatini, 1992; Di Silvio and Padovan, 1998; Di Silvio et al., 2001). As will be shown, some of these processes are very important for a realistic simulation of typical lagoonal features such as salt marshes. Zero-dimensional models based on intertidal concentration have been applied by the Venice Water Authority (*Magistrato alle Acque*) to the Lagoon of Venice to evaluate the effects of man-made interventions, such as dredging, land reclamation, excavation of new canals, construction of jetties etc. The concept has been subsequently extended to a number of semi-empirical models for analogous configurations (De Vriend, 1996; Stive et al., 1998; Wang et al., 1998; Kragtwijk et al., 2004; Townend and Amos, 2008).
The present paper describes a two-dimensional model based on the concept of transport concentration, in order to clarify the main mechanisms controlling the initial planimetric configuration (lagoon ontogeny) and the subsequent bathymetric evolution of tidal lagoons.

2.2 The *transport* (or *tidally averaged*) concentration concept

In a tidal basin sediments are conveyed (mostly in suspension) from the shoals to the channels and through the channels out to the sea during the ebb phase, and are generally moved inward during the flood phase. At the tidal scale (hours) the sediment transport is predominantly advective. It is given by the product of depth-integrated velocity (discharge per unit width, also called water flux) and depth-averaged concentration, while the local longitudinal dispersion (Taylor, or Elder, type) is almost negligible.
At the longer scale (weeks) sediment is mainly transported within the lagoon by the tidally averaged dispersion (several orders of magnitude larger than Taylor's dispersion), while the advective term (Eulerian residual water fluxes) is generally rather small. Another long-term component of sediment transport is due to the asymmetry of the tidal

wave, i.e. to the different durations of the ebb and the flood phases; this gives rise to a residual motion of particles in either the ebb or the flood direction and may be quite important in the channels of some estuaries or lagoons. We will return to these mechanisms in Section 2.4.

Transport (or *tidally averaged*) concentration is defined as the long-term concentration, prevailing in a certain location, which determines the long-term net sediment transport as proportional to the concentration itself (advection) or proportional to its spatial gradient (dispersion).

We may also define a *tidally averaged equilibrium concentration* as the local transport concentration value which, with the prevailing local shear stresses, does not produce net erosion nor deposition.

2.3 Sediment transport and sediment balance

The two-dimensional intertidal balance equation for the sediments over an elementary water column of base $dx\,dy$ and (tidally averaged) depth h_e are written as:

$$\frac{\partial C h_e}{\partial t} + \frac{\partial T_x}{\partial x} + \frac{\partial T_y}{\partial y} = E \tag{2.1}$$

where C is the transport (or tidally averaged) concentration, T_x and T_y are the net sediment transport components (averaged over a significant number of tidal oscillations) in the directions x and y respectively.

E is the long-term entrainment or deposition rate and the first term $\partial C h_e/\partial t$ (the accumulation term, namely the change of transport concentration in the water column) is neglected because it is much smaller than the net exchange with the bottom (Fig. 2.1). The following depth-averaged expressions for the net sediment transport are obtained by integrating the instantaneous suspended transport equations over a long period of

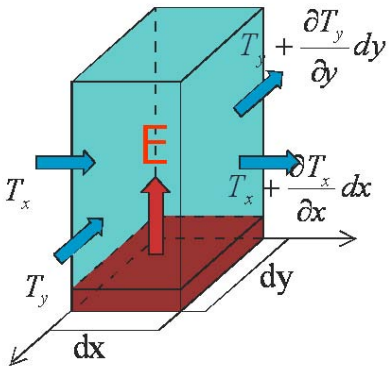

Figure 2.1: Long-term balance of sediment trough an infinitesimal element of the lagoon: T_x and T_y are the net sediment transport, E is the long-term entrainment or deposition rate, dx and dy are the dimension of infinitesimal water column.

time:

$$T_x = h_e \left(C U_R - D_{xx} \frac{\partial C}{\partial x} \right) \tag{2.2}$$

$$T_y = h_e \left(C V_R - D_{yy} \frac{\partial C}{\partial y} \right) \tag{2.3}$$

where U_R and V_R denote the depth-averaged Eulerian residual flow velocities in the x and y directions, and D_{ij} is the tidal dispersion tensor.

2.4 Residual flow, asymmetric tidal flow and tidal dispersion

Eulerian residual water fluxes U_R and V_R are given by integrating the depth-integrated velocities (water fluxes) at tidal scale over a long period of time. Typical residual fluxes are the steady longshore currents along the littoral. In the vicinity of river mouths, Eulerian water fluxes are also due to the river discharges. In general, however, Eulerian

residual water fluxes may also depend on tidal currents. In many lagoons, for instance, residual water fluxes of tidal origin are determined by the interaction of inertial, gravity and friction forces in the tidal channel network. As a consequence, some branches of the interconnected channels convey a larger volume of water during the ebb phase and others during the flood phase.

Residual water fluxes U_R and V_R are found to be markedly different from zero also in front of the three inlets of the Lagoon, which are presently provided with long jetties extending into the sea. In fact, while during the flood tide the velocity pattern in this area is similar to a potential flow, it looks like a turbulent jet during the ebb tide. By combining these two velocity fields (even if the residual flux in the channel within the jetties is perforce equal to zero) a residual circulation arises in the portion of the sea outside the jetties which is oriented in the outward direction along the axis of the inlet and in the inward transversal direction elsewhere. Note that these residual fluxes (which are much less evident in natural inlets) produce a net export of sediments from the lagoon.

Another mechanism which produces a net sediment flux either in ebb or in flood directions is due to the asymmetry of the tidal oscillation. Namely, if the duration of a tidal phase is systematically shorter than the duration of the other one, the corresponding tidal velocity is larger and (due to the strongly non-linear relation) the net sediment transport is not zero, even if the residual water flux is zero. A theoretical analysis of the net sediment transport driven by a non-symmetrical tidal wave and of the consequent morphological effects has been made for convergent estuaries (Lanzoni and Seminara, 2002). If non-uniform bottom material is considered (Di Silvio and Teatini, 1992) a further net sediment flux may be produced by the selective transport of coarse and fine fractions during the slack periods before flood and ebb tide (Dronkers, 1986; Marani et al., 2003; Wang et al., 2002).

Although the sediment flux produced by non-symmetrical tidal wave does not in principle require the presence of a residual water flow, nevertheless it can be formally ac-

counted for by a "virtual" addition $\mathbf{W_A}$ to the residual velocities U_R and V_R in Eqs. 2.2 and 2.3. The vector $\mathbf{W_A}$ has the direction of the faster phase of tidal flow and the intensity of the equivalent tidal velocity multiplied by the relative difference between the average concentration of the two phases. If a non-uniform grain size material is considered, the concentration in ebb and flood tide should be disaggregated in different fractions.

The various components of the residual flow (including the virtual velocity accounting for the tidal asymmetry) can be evaluated by means of the hydrodynamic steady flow model (Section 2.9).

Within the lagoon of Venice, however, the tidal dispersion is the largest component of the long-term net sediment transport. For a tidal lagoon formed by a network of deep channels cut in broad and shallow areas, the dominant mixing mechanism is due to the alternate "trapping and pumping" between channel and shoals during an entire tidal cycle (Schijf and Schönfeld, 1953; Okubo, 1973). To understand this mechanism, let us see how any tracer (not necessarily a sediment) continuously discharged in the lagoon at the landward end of a tidal channel, is gradually transported from here to the sea. In tidal flood conditions clear water enters from the sea to the lagoon basin through the channel. The tracer concentration in the channel is less than in the shoals, so the clear water is transported to the shoals from the channel. On the ebb tide the concentration in the shoals is higher and the tracer is transported to the channel and eventually to the sea. In other words, the presence of the shoals (with a much lower longitudinal velocity) forms during each tidal phase a temporary delay of the tracer particles trapped here with respect to the tracer particles moving in and out along the channel. On the long term, an equilibrium configuration is reached, where there is a net transport of the tracer along the channel equal to the tracer input at the estuary's landward end. At the same time, the longitudinal distribution of the tidally averaged concentration (or "transport concentration") will present a negative gradient from the land to the sea, proportional to

the amount of transported tracer.

The same mechanism applies to suspended sediment if the concentration in the sea is lower than within the lagoon (degrading lagoon). The sign of transport is inverted if the concentration in the sea is higher than within the lagoon (silting lagoon). The tensor of tidal dispersion **D** expresses the physics of this exchange through a square proportionality with the velocity field:

$$\mathbf{D} = k \begin{pmatrix} U_t^2 & 0 \\ 0 & V_t^2 \end{pmatrix} \tag{2.4}$$

Equation 2.4 is an extension to a branching channel network of the hypothesis made by Dronkers (1978) for a tidal basin with a single channel.

The spatial distribution of the dispersion tensor depends on the local velocity, in its turn depending on the planimetric structure of the channel network. It is assumed in this model that the velocity field directions remain basically constant during the tidal cycle. As a consequence the distribution of **D** can be provided by the velocity field U_t and V_t in maximum flood conditions with a representative tidal amplitude (see Section 2.9).

The value of the constant k also absorbs the frequency distribution of tidal currents amplitude over a longer period. A theoretical evaluation for the case of a one directional channel has been made (Dal Monte and Di Silvio, 2004).

2.5 Net erosion rate, subsidence and eustatism

The erosion rate E (eq. 2.1) is expressed by the following first-order reaction equation:

$$E = w_s \left(C_{eq} - C \right) \tag{2.5}$$

where C is the time-averaged sediment concentration and C_{eq} is the equilibrium concentration of the water column (see Section 2.6). The vertical exchange velocity w_s is proportional to the fall velocity w of the equivalent particle size of the bottom material.

The ratio ($w_s/w > 1$) depends in principle on the vertical profile of the concentration and, therefore, on grain size diameter and hydrodynamics (waves and currents). In the present work w_s is considered constant and equal to 0.003 m/sec, reasonably larger than the value of w for the praviling grainsize within the lagoon (about 70 μm). The vertical exchange velocity w_s gives an idea of the rapidity of adaptation of the actual concentration C to the local hydrodynamic characteristics: if $w_s \to 0$, there is no exchange with the bottom ($E = 0$, neutral tracer). If one puts w_s tending to infinity (immediate adaptation), one finds $C \equiv Ceq$ while the dependent variable in Eqs. 2.1, 2.2, 2.3 becomes directly $C_{eq}(x, y, t)$ (Eq. 2.17); this means that the erosion rate E is directly given by the left-hand term in Eq. 2.1.

The long-term variation of the average water depth h_e, including the subsidence and eustatism rate (respectively α_s and α_e) is written:

$$\frac{\partial h}{\partial t} = E + \alpha_e + \alpha_s \tag{2.6}$$

2.6 Equilibrium concentration in channels, shoals and littorals

The transport concentration C at a given location is obtained by averaging the instantaneous concentration $c(t)$ over a long period of time. The instantaneous concentration can be computed by any appropriate transport formula, as a function of the local currents (especially active in the channels) and of the local waves (especially active over the shoals).

As far as currents are concerned, let us consider a monomial transport formula for the sediment transport in suspension, such as Engelund and Hansen (ASCE, 1975), and let us call q_s the volumetric sediment discharge per unit width produced by the water flow,

$$q = v \cdot h \tag{2.7}$$

where v is the water velocity averaged over the water depth h. From the monomial transport equation one finds:

$$q_s \propto v^n \tag{2.8}$$

where $n \approx 5 - 6$, while the instantaneous sediment concentration is:

$$c = \frac{q_s}{q} \propto \frac{v^n}{q} \propto \frac{q^{n-1}}{h^n} \propto \frac{q^4}{h^5} \tag{2.9}$$

where q is the water discharge per unit width of channel. As the duration distribution of the tidal flow is almost linear, by averaging Eq. 2.9 over the year one finds the long-term average concentration in the location:

$$C_c = \frac{f_c q^4}{h_e^5} \tag{2.10}$$

where h_e is the local tide-averaged depth, $q = Wh_e$ is the local maximum water flux with $W = sqrtU^2 + V^2$ and the coefficient f_c is a function of the tidal range and sediment grain size. Both q and f_c are functions of the planimetric characteristics of the location and can therefore be considered rather constant over long periods of time, even if the bottom elevation (local water depth he) is subject to evolution. Eq. 2.10 provides in principle the "equilibrium concentration" due to the tidal currents.

An expression similar to Eq. 2.10 can also be obtained for the long-term average concentration produced by waves, by assuming that the proportionality of Eq. 2.8 still holds if v is the instantaneous orbital velocity produced by the waves near to the bottom (shallow waters) and that v is proportional to q/h. This assumption implies that the alternate sediment flux q_s during the passage of a wave is in phase with the corresponding depth-integrated water flow q. Note that waves do not transport sediments but just stir them: long-term sediment transport on the shoals (as well as in the channels) is produced by tidal dispersion and residual flow acting on the long-term averaged concentration. Under the hypothesis made, the instantaneous concentration on the shoals is:

$$c = \frac{q_s}{q} \propto \frac{v^n}{v \cdot h} \propto \frac{v^{n-1}}{h} \tag{2.11}$$

By evaluating with the linear wave theory the value of the maximum orbital velocity v_m by:

$$v_m = \frac{1}{2}\sqrt{\frac{g}{h}}H_w \tag{2.12}$$

one finds the concentration on the shoals averaged over the wave period:

$$c = k_1 \frac{H_w^{n-1}}{h^{\left(\frac{n-1}{2}+1\right)}} \tag{2.13}$$

with k_1 including all the constants of proportionality. In order to obtain the long-term average concentration in a given location, Eq. 2.13 should be averaged over, say, a few years.

The significant wave height H_w in shallow water, can in its turn be approximately computed by the formula of Bretschneider, simplified to a monomial equation of the type: $H_w = h_s^{0.5} \cdot f$ (fetch and wind characteristics) where h_s is the water depth along the fetch, assumed to be equal to the local tide- averaged depth h_e. The exponent 0.5 appears to be reasonably constant for the conditions of the lagoon of Venice. By integrating the Bretschneider formula over a long period of time and different durations (Dal Monte and Di Silvio, 2004), it is possible to obtain the following expression of the equilibrium concentration produced by waves

$$C_w = \frac{f_w}{h_e} \tag{2.14}$$

where h_e is the local tide-averaged depth and f_w is a parameter depending on local wind velocity and frequency, as a function of its direction, including the fetch length. As q_s (Eq. 2.8) depends on sediment grain size, the values of f_c and f_w tend to decrease for coarser bottom composition. Moreover, an appropriate value of f_w can also account for the enhanced resistance of the bottom due to vegetation, either sea weeds (e.g. Zostera marina) on the shoals or aerial alophile species on the salt marshes.

Eq. 2.14 has been obtained assuming that the averaged depth along the fetch, h_s, is pro-

portional to the local depth (as it is the case within a shallow lagoon). If this assumption is removed (as is the case on the open coast), one finds

$$C_s = \frac{f_s}{h_e^3} \tag{2.15}$$

with the coefficient f_s depending on the littoral wave-climate characteristics.

A long- term value of equilibrium concentration is also present at the mouth of any river flowing in the lagoon or in the sea

$$C_r = \frac{f_r Q^4}{B^4 h_e} \tag{2.16}$$

where Q is the annual average waterflow, B the river width and f_r a constant of proportionality.

Assuming that the concentration produced by currents, local wind and sea waves are given by independent mechanisms, the total equilibrium concentration C_{eq} in any location is obtained in principle by summing up expressions 2.10, 2.14, 2.15, 2.16:

$$C_{eq} = C_c + C_w + C_s + C_r \tag{2.17}$$

With respect to other formulations of the equilibrium concentrations, these expressions are simpler, robust and suitable to point out the effects of the depth distribution $h_e\,(x, y)$. Although the exponents of h_e in these expressions may assume slightly different values (depending upon the empirical formulas used for evaluating sediment transport and wave height) this variations are conveniently absorbed by the coefficients f_c, f_s, f_w which in their turn are susceptible of a relatively easy calibration against morphological data in quasi steady conditions. Indeed, while the general structure and the exponents of Equations 2.10, 2.14, 2.15 and 2.16 depend on the selected transport formula and the Bretschneider formula (Dal Monte and Di Silvio, 2004), the numerical values of f_c, f_w, f_s, and f_r need to be found by comparison with field data.

It is interesting to observe, however, that $C_e q$ in the lagoon is dominated either by waves (on the shallow shoals, where $q \approx 0$), or by currents (in the channels, where C_w rapidly decreases as the depth increases).

2.7 Construction and demolition of salt marshes

Salt marshes are important components of tidal lagoons which are distinguished by a particular definition of the stirring coefficient f_w; from a morphodynamic point of view they are relatively active and changes of their planimetric configuration may affect the fetch distribution all over the entire basin. Although some attempts of modelling the complex behaviour of marshes have been made, a thorough verification of such models is not yet available.

Salt marshes are generally protected by a thick cover of vegetation. As vegetation strengthens to a very large extent the bottom resistance, resuspension of sediments by waves is virtually impossible and equilibrium transport concentration is extremely low or even zero. In other words salt marshes act as a very efficient trap, capturing sediments from the shoals and the channels nearby. Sediments trapped by salt marshes, though subject to consolidation, contribute to the raising of the marsh surface. As the surface rises, water fluxes in the marshes, as well as the corresponding sediment transport, become smaller and smaller. Sediment transport goes practically to zero when the marsh surface approaches the maximum elevation of the tidal range. At this point, a salt marsh remains permanently dry, alophile turns to planitial vegetation and the marsh evolves into an island.

The rising rate of salt marshes is almost invariably limited by the rate of subsidence and eustatism which compensate the capture of sediments. The overall balance of sediments determines not only the elevation, but also the surface area covered by salt marshes. Both elevation and surface area of tidal marshes, then, may start to change again if subsidence/eustatism rates and tidal range are not stationary. To predict salt marshes submersion, also local soil consolidation should be accounted for and appropriate compaction coefficients should be defined.

To simulate the change of the salt marshes area, the collapse of their steep edges needs to be described. In this regard, a simple zero-dimensional geotechnical model has been

proposed (Di Silvio et al., 2001), but not verified against field data. The geotechnical analysis requires a careful revision with regard to the role of vegetation in strengtening the marsh edges. No collapse mechanism, however, has been introduced in the present computation.

Note that the presence of salt marshes may strongly affect the fetch lenght and then the value of f_w in Eq. 2.14. If the biological-geotechnical model is accurate, the appearance and disappearance of salt marshes is properly simulated and any possible variation of f_w (and even of h_e) can be accounted for during the computation in non-stationary condition.

The behaviour of salt marshes in non-stationary conditions (that is when the long-term overall sediment balance is in excess or deficit) presents a strong hysteresis and asymmetry (Di Silvio and Padovan, 1998). In fact, while the construction phase is gradual and controlled by the progressive growth of vegetation, the demolition phase is generally delayed with respect to the sediment deficit as it depends on the collapse of the steep edges. This particular behaviour can be simulated by the long-term morphological model, provided that the biological and geotechnical processes are correctly incorporated.

The role of biology is probably reflected, during the construction phase, also by the type of vegetation initially thriving on the marshes. In presence of large riverine sediment input (it was the case for the Venice lagoon before the XV century), marshes start near the river mouths and are covered by fresh-water species. In contrast, if the sediment is imported mostly from the sea, marshes build-up along the tidal channels near the inlet and their vegetation cover generally is mostly alophile.

The vegetation cover of salt marshes is responsible for other morphological features of tidal lagoons. For example, when the extension of salt marshes is large and local wind waves are relatively small, there is a tendency to form relatively deep zones (ponds) behind the line of salt marshes. This is probably due to the fact that transport concentra-

tion is virtually nil in the salt marshes and, consequently, it is also very low in the zones behind.

Another effect of the low concentration prevailing in the vicinity of salt marshes, is the cross-section geometry of the tiniest creeks that develop over salt marshes. The ratio between the cross-sectional area and the corresponding tidal discharge is much larger for these creeks than for the big channels crossing relatively deep shoals (Rinaldo et al., 1999). This agrees with the fact that the concentration in channels tends to decrease when the extension of salt marshes is larger (Di Silvio and Dal Monte, 2003).

Marsh morphodynamics, in conclusion, is extremely complex as it ensues from the competition of channel flows (generally bringing in sediments) and wind waves in shoals (generally contributing to depth increase and eventual edge demolition). While this model howewer may have all the necessary ingredients incorporated, in the present computation no demolition mechanism has been as introduced, and therefore the marshes extension is only controlled by the sediment input.

The marshes generation has been accounted for, by assuming an appropriate value of C_{eq}, depending on the bottom elevation z_{b0} (below the mean sea level). Whenever the bottom is generally submerged ($z_b > 0.05$ m) C_{eq} is given by Eq. 2.17. When -0.05 m$< z_b < 0.05$ m (about the limit of vegetation) the value of C_{eq} has been assumed varying gradually with elevation from the standard value to 0 and remains equal to zero until $z_b > z_{bt}$ (limit of the highest tide). Analogously when $z_b > -0.30$ m the vertical exchange (adaptation) velocity w_s is equal to 0.03 m/s; when $z_b < -0.30$ m the vertical exchange (adaptation) velocity w gradually decreases to the value of zero (no exchange of sediments); when $z_b = z_{bt} = -0.35$ m (limit of the highest tides), the value of w_s is set equal to zero.

According to the mechanism described above, the equilibrium elevation of marshes is to be found between the highest tide elevation z_{bt} and the lowest elevation z_{bv} compatible with the alophile vegetation, depending upon the values of α_e and α_s. As a matter of

fact, the bottom distribution of the marshes in the lagoon of Venice exists within a quite narrow range.

2.8 Effective water depth

The average water depth in any location of the lagoon is not always given by the value of $h = -z_b$, but depends on the local bottom elevation. In fact, if the annual maximum tidal range is a_m, it follows that, during the year, the bottom is permanently submerged only where $z_b > a_m/2$; by contrast the bottom is never submerged where $z_b < -a_m/2$, while we have an intermediate submergence for values in between. If we assume that the frequency distribution of the tidal range is linear, we may obtain the value of the effective water depth h_e at each location of the lagoon, by multiplying the local value of h by the submergence period of the tide. One finds:

$$h_e = \begin{cases} h = -z_b & \text{if } z_b \geq a_m/2; \\ \eta_0 \left[1 - \frac{1}{2}\left(1 - \frac{h}{\eta_0}\right)\right]^2 & \text{if } -a_m/2 < z_b \leq a_m/2; \\ 0 & \text{if } z_b < -a_m/2. \end{cases} \tag{2.18}$$

The effective value of h_e should be used instead of h, in every equation of the model.

2.9 Hydrodynamic submodel

As it has been repeatedly observed, there is no need for the present model to calculate the alternate water flow at tidal time-scale. A hydrodynamic submodel, however, is required to describe the velocity field in maximum flow conditions and to calculate the residual Eulerian currents.

In particular, the velocity field in maximum flow conditions U_T and V_T is necessary for the computation of the tidal dispersion tensor $\mathbf{D}$ (Eq. 2.4) and the equilibrium concentration C_c for the tidal currents (water flux q in Eq. 2.10). The velocity field for the

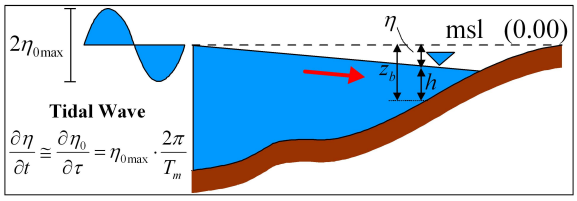

Figure 2.2: Water level at maximum flood conditions: h is the local water depth, z_b is the bottom elevation below the mean sea level, $\eta = z_b - h$ is the local surface deviation from the mean sea level, η_0 is the water level at the sea, $\eta_{0,max}$ = -0.35 m is the maximum tidal elevation, h is the local water level

residual Eulerian currents is necessary for the computation of the long-term convective components, considering all the possible causes of residual currents U_R and V_R (steady longshore currents; fluvial currents; jetties included currents, etc.); plus the virtual currents W_A (proportional to the tidal currents) taking into account the possible asymmetry of the tidal oscillation.

It should be recalled that the linear hydrodynamic model provides a value of (U_T,V_T) in maximum flow conditions sufficiently correct to calculate $\mathbf{D}$ and C_c, but cannot directly reproduce any asymmetry of the tidal wave.

The velocity field in maximum flow conditions and the velocity field for the residual Eulerian fluxes have different applications and should be considered separately. Both velocity fields, however, can be determined (with appropriate boundary conditions) by the same waterflow equations (2.19), (2.20), (2.21), namely the 2-D shallow water equations of stationary flow. Simplifications introduced in the models are a bit less severe than the ones yelding the dimensionless Poisson form obatained by Rinaldo et al. (1999). In order to reproduce the ontogenesis of both tidal channel and shoals, in fact, the hypothesis of almost constant depth of shoals has been relaxed.

Under the hypothesis of “short” tidal lagoon (with propagation time between inlet

and lagoon basin lower than a quarter of a tidal period T_m), it can be assumed that at maximum flood conditions (Fig. 2.2) friction terms dominate, inertial effects are negligible compared to friction terms in the momentum equation and that the vertical rate of change of tidal elevation ($\partial\eta/\partial\tau$) is constant all over the basin (and equal to the rising velocity in the sea) in each part of the lagoon. By linearizing the friction term, analytical treatment leads to the following expressions for the velocity components along the $x-$ and $y-$ directions (U_T and V_T respectively) and for the tidal elevation:

$$U = -\frac{h^2\chi^2}{W_T}\frac{\partial\eta}{\partial x} \tag{2.19}$$

$$V = -\frac{h^2\chi^2}{W_T}\frac{\partial\eta}{\partial y} \tag{2.20}$$

$$-\frac{\partial}{\partial x}\left[\left(\frac{-h^2\chi^2}{W_T}\right)\frac{\partial\eta}{\partial x}\right] - \frac{\partial}{\partial y}\left[\left(\frac{-h^2\chi^2}{W_T}\right)\frac{\partial\eta}{\partial y}\right] = \frac{\partial\eta}{\partial t} \tag{2.21}$$

where χ represents the Chézy coefficient and $W_T = \sqrt{U_T^2 + V_T^2}$; f represents a distributed injection/extraction term which is equal to $\eta_{0,max}2\pi/T_m$ in the tidal flow equation.

2.10 Model structure and numerical matters

The model computes hydrodynamic quantities, sediment transport and bottom evolution, all under the hypothesis that the processes can be represented as successions of steady states. The calculation follows an iterative procedure, whose main steps are described below.

The cycle starts from the geomorphological configuration, which can be provided either as an initial condition or as the result of the previous iteration, and is used in the calculation of the hydrodynamic quantities.

The hydrodynamic submodel is subdivided into two modules: one referred to the tidal

motion field and one to the residual Eulerian fluxes (see Sec. 2.9). The quantities calculated in the tidal module are used for the determination of the tidal dispersion tensor, while the residual Eulerian velocities are required for the computation of the advective transport component. Both tidal and residual velocities contribute to the calculation of q and the equilibrium concentration, C_c (Eq. 2.10). The numerical solution of the hydrodynamic non-linear problem is obtained by applying an under-relaxation scheme to the Finite Element Galerkin discretization of Eq. 2.21; the convergence of the scheme is accelerated by taking as a first trial velocity field the one computed at the previous time step.

After the hydrodynamic module and the calculation of the related quantities, it is possible to solve the sediment transport equation. The numerical solution is obtained with a Finite Element Streamline Upwind Petrov-Galerkin method, in which a proper weight added to the base function introduces an anisotropic corrective diffusion in order to stabilize the scheme with respect to numerical effects potentially induced by the advection term.

The bottom evolution is calculated as

$$\Delta z = w_s \left(C_{eq} - C \right) \Delta t \tag{2.22}$$

where the time step is chosen in order to allow a sufficient resolution in the description of morphodynamic processes and to avoid numerical instabilities.

2.11 Model setup and applications

It has been supposed that the generation of the lagoon is determined by the formation of a large breach in the littoral dunes and consequent invasion by the sea of the alluvial plain lying behind them.

The model has been applied to a schematic system consisting of an expanse of sea, inlet area and a lagoon basin. In the sea expanse the interactions between tidal currents,

longshore currents and sea waves (namely the formation of the outer delta) takes place. The lagoon basin may also include a fluvial mouth and the terminal part of the river flowing across the alluvial plain and through the littoral dunes. In all the simulations, the initial bottom bathymetry in the sea has been assumed linearly increasing along the longitudinal direction seaward, while two different initial configurations (uniform bottom and flat plain with a pre-existing riverbed) have been used for the lagoon basin. At the seaward boundary a local equilibrium concentration has been imposed (Dirichlet conditions), and the boundaries enclosing the lagoon have been assumed impermeable (Neumann conditions) and inerodible. The presence of a river with constant sediment concentration has been also represented with Dirichlet conditions, while the tide propagation in the river is described as an outgoing discharge proportional to the fluvial tidal prism.

Many simulations have been carried out for a sensitivity analysis of various parameters and in order to study the effect of different boundary conditions on the planimetric and bathymetric evolution of the lagoon.

Three different triangular meshes have been tested in order to find a satisfactory trade-off between spatial resolution and computational efficiency.

In the present tests the following parameters have been set as it follows:

- Tidal dispersion tensor coefficient k: 2550 s;
- Vertical exchange (adaptation) velocity w_s: 3.00E-3 m/s;
- Equilibrium concentration coefficients:
  - f_c (tide): 1.08E-3 m^5;
  - f_w (wind): 2.00-4.00E-6 m (for a sensitivity analysis);
  - f_s (sea): 0-1.02E-2 m^3 (at the open sea boundary, decreasing to zero inside the lagoon);

  - f_r (river): 1.60E-3 m;

- Tidal range $\eta_{0,max}$: 0.35 m;
- Tidal period T_m: 43200 s;
- Chézy coefficient χ: 50 $m^{1/2}/s$ constant in the lagoon, 35 $m^{1/2}/s$ near the inlet vertical walls;
- River equivalent discharge Q_r: 115 m^3/s;
- River average concentration C_r: 5.00 ppm;
- River tidal prism: $(100 \times 10000 \times 0.35) = 350000$ m^3;

Eustatism and subsidence phenomena have not been considered ($\alpha_e = \alpha_s = 0$).

2.12 Results and discussion

Some preliminary results are presented here with the purpose to illustrate the performance of the model and to evaluate the effects of the main active mechanisms. The effects of different mesh size can be seen in Fig. 2.3. As expected, the finer the mesh size, the longer the required computational time. Although the global parameters at basin scale (space-averaged depth, space-averaged concentration and total transport through the inlet) do not present strong variations by changing the mesh size, the difference is obviously remarkable as far as the size of the channel network is concerned, especially for the smallest branches which cannot of course be wider than the mesh size. Consequently, for the smaller branches in the lagoon it may be advantageous to use as fine a mesh as practical.

The importance of the net convective transport with respect to the intertidal dispersive transport is shown in Fig. 2.4. This influence is known to be dominant in the

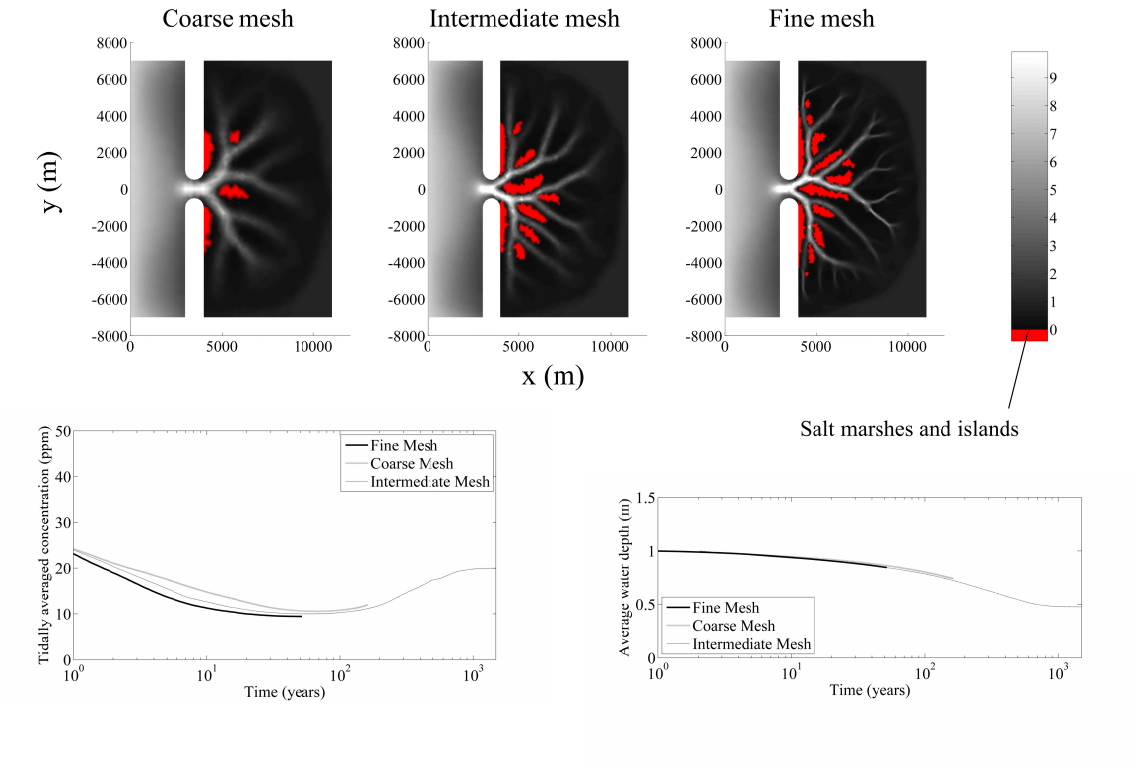

Figure 2.3: Comparison among computations carried out with different mesh size; ontogenesis and earlier long-term evolution with only dispersive transport (no river input). Elapsed time: 50 years. Water depth is expressed in meters.

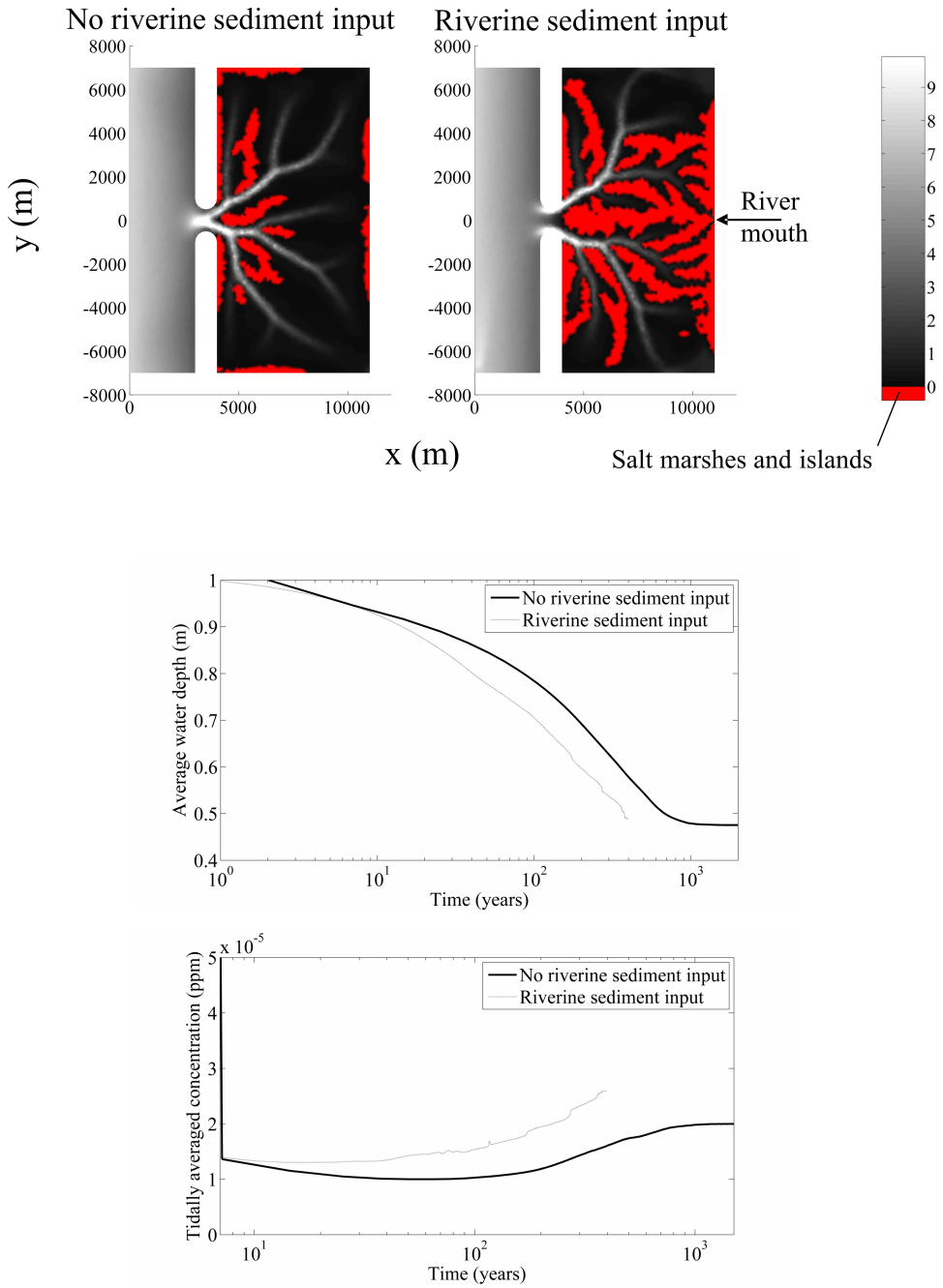

Figure 2.4: Comparison between computations carried out without and with riverine sediment input. Intermediate mesh size (200 m). Computations with riverine sediment input include also South-North longshore currents (about 6 cm/s). Elapsed time: 400 years. Water depth is expressed in meters.

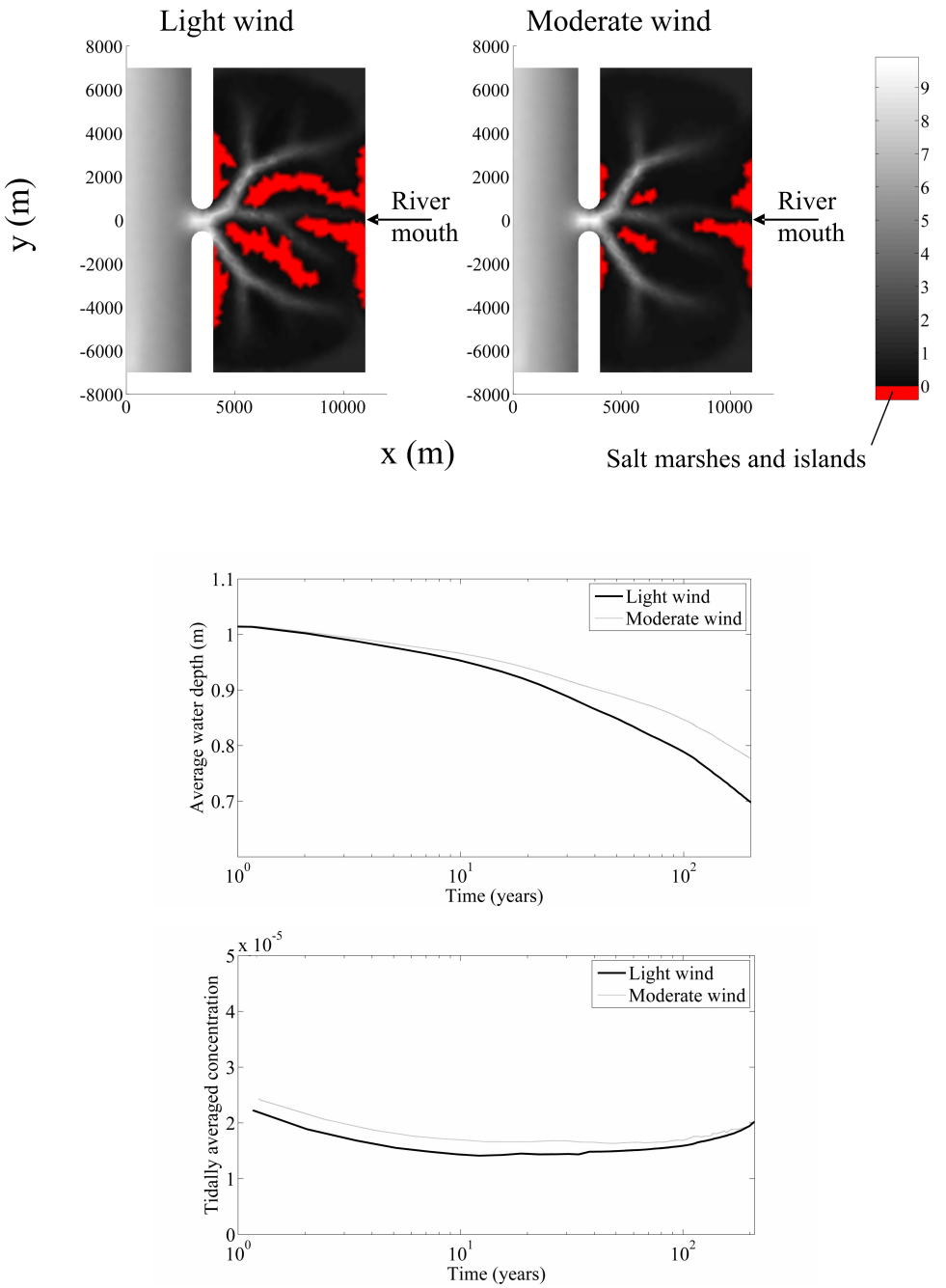

Figure 2.5: Comparison between computations carried out with light and moderate wind. Both computation have been carried out with riverine input and longshore currents (and coarse mesh size). Elapsed time: 200 years. Water depth is expressed in meters.

present lagoon of Venice after the diversion of rivers operated several centuries ago. The convective transport components considered here consist of the input of water and sediments from the river and in littoral longshore currents present along the northern Adriatic coast. As shown in the plan view of the schematic lagoon, the main effect of the river flowing into the lagoon is the rapid formation of an ample expanse of salt marshes near the river mouth, comparable to the expanse of marshes near the lagoon inlet. Apart from the different origin of the material forming the marshes (respectively transported by the river or eroded from the pre-existing alluvial plain and supplied by the sea), one may also observe a certain difference of the channel network configuration in the two areas, branching out from the inlet or from the river mouth. Besides the larger marshes area, an appreciable difference is observed in the evolution of the other overall parameters (average water depth and average intertidal concentration), due to the larger input of sediments into the lagoon from the river mouth.

The asymptotic configuration of the lagoon in Fig. 2.4 has been attained only for the sole dispersion transport (after about 1000 years) and corresponds to a uniform intertidal concentration in the lagoon (equal to the prescribed conditions in the sea C_{sea} =20 ppm). Due to excessive computer time, required by the convective fluxes, the computations in the presence of fluvial sediment input, has been interrupted after 250 years; one may infer however, that the asymptotic equilibrium configuration of the lagoon will exhibit in this case a smaller water depth (in both channels and shoals), corresponding to a value $C = C_{eq}$ quite larger than the boundary condition in the sea. The negative gradient from the lagoon to the sea will conform to the dispersive component of the net sediment transport which conveys the fluvial sediment input out of the lagoon.

Fig. 2.5 shows the effects of wind intensity. To aid comparison, two values of f_w (Eq. 2.14) have been selected, uniformly distributed all over the lagoon, respectively equal to 2E-6 m (light wind) and 4E-6 m (intermediate wind). With the stronger wind, the sediment re-suspension increases and the transport of sediments from the lagoon to the

sea is larger, much as expected. Consequently the extent of the salt marshes surface, especially near the inlet, is strongly reduced by the intermediate wind.
For lack of time, also in this case the computation has been interrupted before reaching the asymptotic conditions. It may be inferred however that, even at the equilibrium, the effect of the wind intensity on the lagoon bathymetry (average water depth) is less apparent than it is on the planimetric configuration. With a more extensive application of the model, it would also be interesting to evaluate the asymptotic (equilibrium) area of the salt marshes (-0.35 m$< z_b < 0.00$ m) and of the islands ($z_b \leq -0.35$ m, never submerged), depending on the various forcing factors: tidal range, wind, sediment input etc.

2.13 Conclusions

The most recent numerical results reported in the present paper allow for the following concluding remarks.

1. For the various configurations that have been considered, it was found that the planimetric evolution of the channel network (lagoon ontogeny) was much faster than the bathymetric evolution of the lagoon bottom.

2. The model appears to be both flexible and robust. A new forcing factor (e.g. the water and sediment input from the river or the long shore littoral currents) can be easily introduced in the model without dramatic or unexpected changes of the model response, both for the planimetric (ontogenic) and the bathymetric evolution phases. Also entirely plausible are the differences exhibited by the model when the mesh size is changed. When the finest network of small channels and the tidal creeks should be locally represented, a zooming technique limited in time and space may be applied.

3. For a realistic representation of the modified supply of sediments from the rivers and from the sea undergone by the lagoon of Venice during the centuries, some components are necessary. First of all, the geotechnical mechanisms of the marsh edge collapse should be implemented for reproducing the reduction of the marshes area. Secondly, the convective components of sediment transport, although rather demanding in terms of computer time, appear to be crucial for an accurate description of the rivers flowing into the lagoon, as well as for simulating the asymmetric flow in front of the inlets when they are provided with jetties.

Chapter 3

Morphodynamic modelling of a tidal basin in presence of graded sediments

3.1 Introduction

Morphodynamic processes in complex coastal and estuarine systems are the result of sediment transport phenomena of different origin and at different time and space scales. Since a complete description of all the processes is actually unfeasible both for practical (enormous requirements in terms of computational effort, overparameterization) and conceptual (several phenomena are still unexplained) reasons, some simplifications of the system conceptualization or of the basic equations are necessary.

Different approaches have been developed endevouring this goal. Lanzoni and Seminara (2002), for example, provided a one-dimensional solution for the evolution and the equilibrium of tidal channels by combining de Saint Venant equations for the tide propagation and Exner equation for the bottom evolution. Townend (2010) formulated an idealised model in which the plan form and the tranversal profiles of an inlet can be predicted by means of equilibrium considerations, only depending on exogenous (or *a priori* definable) forcing factors; the model has recently been applied (Townend, 2011)

to a number of estuaries different for dimension and external constraints. Karunarathna et al. (2008) proposes a behaviour-oriented approach based on the observation of the morphological evolution of an estuary over some decades and the definition of the sediment transport via the solution of an inverse dispersive problem. It is also possible to face the problem in terms of *Transport Concentration* (defined as the long-term averaged sediment concentration in a given location), provided in principle by the balance between the horizontal transport processes and the vertical exchanges between the water column and the bottom. Zero-dimensional examples of this approach are provided by Di Silvio (1989); Stive et al. (1998); Di Silvio et al. (2001); Jeuken et al. (2003).

By associating the concept of transport concentration to the concept of *Equilibrium Concentration* (Dal Monte and Di Silvio, 2004) (namely the time-averaged concentration corresponding, in case of homogeneous sediment, to zero long-term horizontal and vertical net fluxes) and with the further definition of a *Tidal Dispersion* effect (Di Silvio and Padovan, 1998), a two-dimensional vertical-averaged morphodynamic model (from now on referred to as the *Intertidal Model*) was recently developed by Di Silvio et al. (2010) which was able to reproduce the genesis and the evolution of a tidal lagoon by taking into account, albeit schematically, for the combined effect of tidal currents, eulerian residual currents and waves. The flow field was described in a simplified way by means of a steady flow submodel: this allowed the computation of the equilibrium concentration and the tidal dispersion tensor and consequently the mutual interactions between hydrodynamic and morphodynamic processes. The Intertidal Model is able to reproduce such phenomena as the development of a dendritic channel network and the formation and destruction of tidal marshes.

In the present paper a further extension of the Intertidal Model is introduced in order to deal with mixed non-cohesive sediments of different size. After a description of the mathematical framework of the model, some attention will be paid to the expressions of equilibrium concentration and their implications from the modelling point of view.

The description of some simulations will follow, and some considerations will be drawn about the factors leading to sediment sorting and segregation within a basin. A proper understanding of these processes is crucial for a better interpretation of the present state of tidal systems as a result of geological and anthropogenic facts, as shown in Bonaldo and Di Silvio (2011b) where the model presented here has been applied.

3.2 Model formulation

The Intertidal Model presented in Di Silvio et al. (2010) is based on the concept of equilibrium concentration. Depending only on the local mechanisms of sediment entrainment this quantity is, to a certain extent, more controllable than the transport concentration; nevertheless its quantification is relatively straightforward only if the water flows responsible for sediment motion (e.g. tidal currents and waves) are caused by driving forces with no or negligible interaction (Dal Monte and Di Silvio, 2004); this assumption, which will be maintained throughout all the present work, makes possible to treat the equilibrium concentration as an additive quantity; for each driving force it is possible to obtain a simple expression for the related contribution by means of an appropriate manipulation of the Engelund-Hansen formula (ASCE, 1975).
Due to the non-linearity and temporal variability of the processes involved in sediment resuspension and transport, averaging Engelund-Hansen Equation over time can lead to inaccurate and inevitably complicated results: moreover, it should be pointed out that such equation has been obtained with reference to uniform flow conditions, which is not the case of the systems under investigations. Nevertheless, it is possible to retain the main features of the equation by separating the geometric magnitude (namely the depth) from the quantities related to the erodibility of the bottom and the erosivity of the flow. These quantities are synthetically lumped together in a *stirring coefficient* which will need to be calibrated, eventually with an explicit dependence on some hydraulic quan-

tities, where available.

In the present paper, the model introduced by Di Silvio et al. (2010) will be generalized by considering several classes of sediments with granular behaviour. This assumption does not imply that only sand and gravel must be treated, but rather that the sand (or gravel) content of a sand-mud mixture is high enough to give it a granular behaviour (Van Ledden et al., 2004a). The Transport and Equilibrium Concentration will then be defined with reference to every $i-$th grain class, as C_i and $C_{eq,i}$ respectively.

The horizontal transport considered by the model is the sum of a *Tidal Dispersion*, namely the long-term effect of an appropriate number of time-integrated tidal cycles (Schijf and Schönfeld, 1953; Okubo, 1973; Dronkers, 1978), and a *Convective Transport*, which can be given for example by residual eulerian currents or long-shore littoral drift. However, in this study we focus on a tidal lagoon without considering the outer littoral, and although a riverine input will be introduced in some cases, we hypothesize that the transport effect of the fluvial current is generally negligible when compared to the tidal fluxes (*a flea compared to an elephant*, sentenced in the sixteenth century the Venetian hydraulic engineer Cristoforo Sabbadino about the discharge of the river Brenta, at his time flowing into the central basin of the lagoon of Venice). For this reason, their contribution to net sediment transport is not considered, while we represent their effect in terms of sediment resuspension. The tidal dispersion is controlled by a tensor $\mathbf{D}$ whose diagonal terms are proportional to the square power of the $x-$ and $y-$components of the velocity field in maximum flood conditions, U_t and V_t respectively.

$$\mathbf{D} = k \begin{pmatrix} U_t^2 & 0 \\ 0 & V_t^2 \end{pmatrix} \tag{3.1}$$

the proportionality coefficient k is a calibration parameter including the effect of all the variables which can not explicitly be accounted for. A study performed by using a simplified model of a tidal channel-shoal system (Di Silvio and Fiorillo, 1981) qualitatively similar to the Venice lagoon suggest a value of the dispersion coefficient as

formulated by Dronkers of hundreds m^2/s. Since the characteristic velocity in the channels is roughly 1 m/s, this result implies an estimate of k of the order of magnitude of hundreds s. More recently, Tonetto (2009) obtained similar values by comparing the results produced by a short-term detailed model (Delft3D) and a long-term model based on the concept of (inter)tidal dispersion. In this work, the estimate of the value of k was based on the calculaton of a "half concentration time" for a tracer initially uniformly distributed all over a schematic basin, using Delft3D results: such time has been used to identify the value of k, for sake of simplicity assumed constant and uniform, that halves the spatial average concentration within the basin when used in the (inter)tidal dispersion model.

Similarly to what has been shown in Di Silvio et al. (2010), the transport equation for each class, considering in general the presence of the long-term convective velocity $\mathbf{W_R}$ (related to residual currents), can then be obtained by performing a mass budget within the water column, yelding:

$$\nabla \mathbf{W_R} h C_i - div\left(\mathbf{D} h \nabla C_i\right) = w_{s,i}\left(\beta_i C_{eq,i} - C_i\right) \tag{3.2}$$

where h is the *effective depth*, namely the water depth weighed with the submergence time (Di Silvio et al., 2010), and $w_{s,i}$ is the vertical exchange coefficient, proportional to the particle fall velocity and related to the equilibrium concentration $C_{eq,i}$, as defined by Armanini and Di Silvio (1988). Note that the dispersion tensor, depending on the flow field alone, is the same for all the classes. The equilibrium concentration is given by the sum of the contributions of tidal and residual currents, and of sea and internal waves (with their stirring coefficients f_i^k), all corrected with a factor which takes into account the increase of bottom erodibility due to the bed slope $\alpha_{bot,i}$ compared to the repose angle ϕ_i:

$$C_{eq,i} = \left(f_i^{tc}\frac{q_{tc}^4}{h^5} + f_i^{rc}\frac{q_{rc}^4}{h^5} + \frac{f_i^s}{h^3} + \frac{f_i^w}{h}\right)\frac{1}{1 - \frac{\tan\alpha_{bot,i}}{\tan\phi_i}} \tag{3.3}$$

q_{tc} and q_{rc} are the specific discharges for the maximum tidally averaged and residual currents respectively, to be computed by a separate waterflow submodel (Di Silvio et al., 2010). A quantification of the stirring coefficients will be provided in Sec. 3.5.

The material of each class put in suspension by channels and waves, quantified by Eq. 5.1, is transported all over the domain by tidal dispersion and residual currents (Eq. 4.2). While outside the lagoon the convective transport due to sea waves may even become dominant with respect to the tidal dispersion, it can be neglected -as already observed- within the lagoon and in the proximity of the inlet. It should be remarked, however, that within and near the inlet sea waves still play a crucial role for the sediment resuspension (see Sec. 3.5).

The bathymetric change is the sum of subsidence and eustatism rates (α_s and α_e) and the net erosion E, given in its turn by the sum of the net erosion for each class, namely the right-hand term in Eq. 5.1:

$$E_i = w_{s,i}\left(\beta_i C_{eq,i} - C_i\right) \tag{3.4}$$

Hence:

$$\frac{\partial h}{\partial t} = \alpha_s + \alpha_e + \sum_i E_i \tag{3.5}$$

The hydrodynamic submodel solves, under the hypothesis of short tidal basin and instantaneous propagation of the tidal wave, a simplified version of the 2-D Shallow Water Equations in which the inertial terms are neglected (Di Silvio et al., 2010; Bonaldo et al., 2010).

Being the sediment no more uniform, a further sediment budget is required in the mixing layer (whose thickness is represented as δ), beside the one performed in the water column, to describe the time variation in the bottom composition (Di Silvio and Padovan, 1998):

$$\frac{\partial\left(\beta_i \delta\right)}{\partial t} = -E_i + \beta_i^* \sum_i E_i \tag{3.6}$$

β_i^* represents the fraction of the $i-$th class in the zone involved in the vertical fluxes, which can be either the mixing layer or the underlying zone, depending whether a net deposition or a net erosion is taking place.

3.3 Equilibrium Concentration

The key parameters of the model are the dispersion tensor (Eq. 3.1) and the equilibrium concentration (Eq. 5.1). While the former, as mentioned in Sec. 3.2, has already been estimated with an order of magnitude of some hundreds to one thousand m^2/s, the latter requires some more consideration.

First of all let us observe that, apart from the correction due to the bed slope, Eq. 5.1 coincides with the expression of equilibrium concentration already found for a uniform diameter (Di Silvio et al., 2010). In the case of graded material, however, it is convenient to define the stirring coefficients by making explicit their dependence on the respective diameter. This result immediately follows by observing that many monomial formulae (e.g. Engelund-Hansen) show the solid discharge per unit width $q_{s,i}$ conveyed by a stream in equilibrium being proportional not only to the 5th power of the flow velocity but also inversely proportional to the grainsize d_i:

$$q_{s,i} \propto \frac{v^5}{d_i} \tag{3.7}$$

Following the same reasoning (Dal Monte and Di Silvio, 2004), for formulating the representative flow velocity v in the cases of tidal currents, external (sea) waves and internal (wind) waves, one may express the stirring coefficients in Eq. 5.1 as:

$$f_i^{tc} = f^{tc}/d_i \quad ; \quad f_i^{rc} = f^{rc}/d_i \quad ; \quad f_i^{s} = f^{s}/d_i \quad ; \quad f_i^{w} = f^{w}/d_i \tag{3.8}$$

Note that Eq. 5.1 shows that the equilibrium concentration of a certain grainsize depends explicitly on the particle diameter d_i and on the local depth h, while the quantities f^k depend on the specific k-th stirring mechanism. The stirring coefficients f^{tc} and f^{rc}

related to the currents are assumed to be substantially constant all over the domain (lagoon and littoral); by contrast the stirring coefficients for waves f^s and f^w, have quite different values depending on the site conditions. For example, we may assume f^s to be constant along the littoral, where the same meteomarine conditions prevail, with its value that rapidly decaying through the inlet from this value down to zero within the lagoon. On the contrary, the value of f^w may vary remarkably over the shoals, depending upon the direction, intensity and duration of the local wind and, above all, upon its fetch.

It is relevant to observe that, depending on the location, not all the stirring factors f^k expressed by Eq. 5.1 are simultaneously effective: for example, f_s and f_w are nil respectively within and outside the basin, while advective currents are often negligible ($q_{rc} \approx 0$). This circumstance is useful for the numerical quantification of f_k.

3.4 Long-term Morphodynamic Equilibrium

We may define as long-term *morphodynamic equilibrium* of a tidal basin the configuration of the system corresponding to the stationary solution of Eqq. 4.2, 5.1, 3.4, 5.3 and 4.4. This means that both the bathymetry and the bottom composition of the basin, averaged over a number of years, namely $h(x, y)$ and $\beta_i(x, y)$, do not evolve: it must be noted that this definition of (*dynamic*) equilibrium is compatible with the presence of non-zero horizontal fluxes (Townend, 2011). If one assumes, moreover, that the residual convective transport is negligible with respect to tidal dispersion, while subsidence α_s, eustatism α_e and morphological evolution $\sum E_i$ are negligible, one also finds (Eq. 4.2) that horizontal sediment fluxes in the lagoon and through the inlet must be zero, while the concentration must be constant in every location of the domain and equal to:

$$C_i = \beta_i C_{eq,i} \tag{3.9}$$

The constancy of C_i and $C_{eq,i}$ in these conditions imply that the grainsize distribution β_i should also be constant. By rewriting Eq. 5.1 with Eqq. 3.9 and 3.8 one finds:

$$C_i = \beta_i C_{eq,i} = \frac{\beta_i}{d_i}\left[f^{tc}\frac{q_{tc}^4}{h^5} + f^{rc}\frac{q_{rc}^4}{h^5} + \frac{f^s}{h^3} + \frac{f^w}{h}\right] \tag{3.10}$$

Eq. 3.10 gives the value of β_i for each class:

$$\beta_i = \frac{d_i C_i}{\left[f^{tc}\frac{q_{tc}^4}{h^5} + f^{rc}\frac{q_{rc}^4}{h^5} + \frac{f^s}{h^3} + \frac{f^w}{h}\right]} \tag{3.11}$$

if the corresponding constant values of $C_i = \beta_i C_{eq,i}$ (independent boundary conditions at the open sea) are known.

Under these hypotheses, Eq. 5.1 expresses the relationship between the stirring coefficients and the local depth h, considering that the unit water discharges q_{tc} and q_{rc} depend exclusively on the planimetric configuration of the basin. This implies that it is also possible to evaluate from Eq. 3.10 the value of the (simultaneously active) stirring coefficients f_k by direct inspection of the entire computational domain, assumed to be in equilibrium conditions with no horizontal sediment fluxes.

While the hypothesis of negligible values of α_e, α_s, and $\sum E_i$ (with respect to the ratio G_S/S_b between the sediment flux G_S exchanged by the computational domain with the outer world during a tidal cycle and its horizontal surface area S_b) is very often satisfied both within the tidal basin and over the adjacent littorals, the hypothesis of negligible net convective flux (with respect to tidal dispersion) is very likely acceptable only for the lagoon proper, as the long-shore and cross-shore sediment transport are definitely prevailing outside. It is therefore convenient limiting the computational domain to the sole tidal basin, including the inlet area, also considering that the long-term (net) sediment transport mechanisms in the littoral area have not so well been investigated.

3.5 Boundary conditions at the inlet

While the values of C_i and β_i at the open sea can legitimately be considered as external and independent boundary conditions, the concentrations and bottom composition at the inlet depend somehow both on the littoral dynamics and on the inlet configuration. Herewith the assumption has been made that in the lagoon inlet only the tidal currents and the sea waves are active as stirring mechanisms and that the quasi equilibrium hypotheses discussed in the previous section are satisfied. Namely we may assume that, in the inlet, Eq. 3.10 may be rewritten as:

$$C_i = \beta_i C_{eq_i} = \frac{\beta_i}{d_i}\left[f^{tc}\frac{q_{tc}^4}{h^5} + \frac{f^s}{h^3}\right]\frac{1}{1-\frac{\tan\alpha_{bot}}{\tan\phi}} \tag{3.12}$$

In particular, if the inlet is protected by jetties (and therefore sheltered from wave propagation, narrow and deep) we may assume that $f^s = 0$ (only currents active). By contrast, along a littoral near the shoreline only sea waves are active, and therefore $q_{tc} = 0$.
For the calibration of the coefficients f^{tc} and f^s an analysis of field data was made, with reference to Venice Lagoon and North-western Adriatic Sea. To this aim it was made use of data sets containing information about suspended sediment time-averaged concentration in the Lido Inlet (Northern lagoon) and the neighbouring littoral, provided by the Venice Water Authority and CORILA (Magistrato alle Acque di Venezia and CORILA, 2006), and a detailed survey performed by Brambati et al. (1977), in which the near-shore bottom composition of the Adriatic Sea between the rivers Brenta and Tagliamento was analized.
The averaged suspended concentration C_{LIM} recorded at the LIM turbidity meter, h_{LIM} =9 m below the mean sea level a few kilometers north of the Lido inlet, was equal to 20 ppm, while the bottom composition was known for depths from 1 to 8 meters and extrapolated to h_{LIM} (Tab. 3.1). By considering that the only sediment resuspension factor along the littoral was the effect of sea waves, and equating $\sum_i \beta_i C_{eq,i} = C_{LIM}$ one can

obtain an algebric equation in the only unknown f^s.

$$f^s = \frac{C_{LIM} h_{LIM}^3}{\sum_i \beta_i / d_i} \tag{3.13}$$

Within the present Lido inlet, protected by jetties, the assumption was made of sediment resuspension given by the effect of tidal currents alone. For the calculation of f^{tc} the averaged suspended concentration for each class C_i recorded by the turbidity meter LMR at a depth of h_{LMR} =9.5 m was used. One finds:

$$f^{tc} = \frac{h_{LMR}^5}{q_{tc}^4} \sum_i C_{i,LMR} d_i \tag{3.14}$$

The results of the calibration are shown in Table 3.2, where measured and computed granulometric curves for bottom and suspended sediment are shown in Figg. 3.1 and 3.2. It must be noted that, while in the present conditions the contribution of sea waves is neglible inside the inlet (in this case the value of f^s is set to zero throughout the whole basin), even without jetties its value could be assumed to be rapidly decreasing through the inlet (Bonaldo and Di Silvio, 2011b).

When a tidal basin is represented without considering the outer sea reach, it is necessary to impose the boundary conditions at the inlet. Within the conceptualization shown in this Section, it can be considered that the reference suspended concentration is the one corresponding to the highest isobath of the undisturbed littoral which can be found in front of the inlet. This means for example that such interventions like the contruction of jetties at the inlet actually change the boundary conditions for the system, by displacing the interface between the basin and the sea towards a deeper zone with finer sediment and smaller suspended concentration.

3.6 Model application

The model has been implemented in a finite element scheme (Di Silvio et al., 2010) and applied to a schematic basin of 10x17 km, discretized in a triangular mesh with a char-

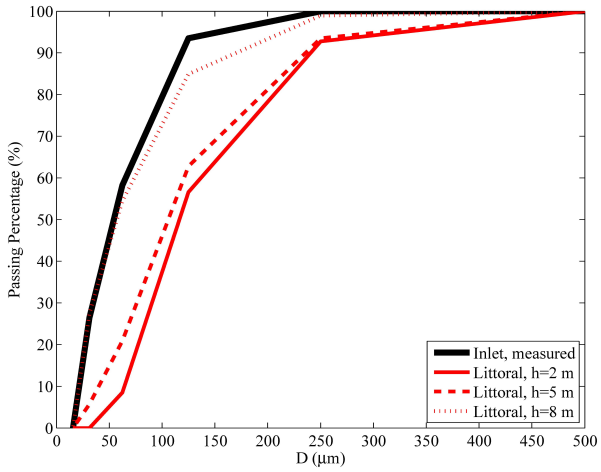

Figure 3.1: Comparison between measured suspended concentrations at Lido inlet and calculated suspended concentrations on the littoral

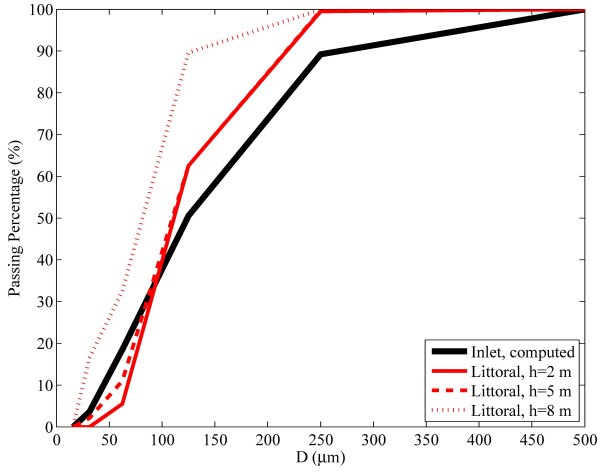

Figure 3.2: Comparison between measured bottom composition on the littoral and computed bottom composition at the Lido inlet

acteristic dimension of about 250 m. Dirichlet conditions (prescribed concentration) were set at the inlet, while the river mouth was modeled, when present, with Neumann

	class, d_i (μm)					
depth (m)	**1**	**2**	**3**	**4**	**5**	**6**
	15.6	31.3	62.5	125	250	500
1	0	7.50e-3	2.15e-1	4.92e-1	2.85e-1	5.00e-4
2	0	2.75e-2	3.13e-1	4.70e-1	1.87e-1	2.50e-3
3	0	2.75e-2	3.18e-1	4.72e-1	1.82e-1	5.00e-4
4	1.02e-2	3.23e-2	3.64e-1	4.67e-1	1.26e-1	5.00e-4
5	1.04e-2	5.51e-2	3.02e-1	4.44e-1	1.87e-1	1.50e-3
6	5.01e-2	8.74e-2	3.17e-1	4.12e-1	1.33e-1	5.00e-4
7	8.77e-2	1.13e-1	3.74e-1	3.86e-1	3.88e-2	5.00e-4
8	8.25e-2	1.63e-1	3.65e-1	3.37e-1	5.20e-2	5.00e-4

Table 3.1: Bottom composition $\beta_i\,(d_i)$ on the littoral (extrapolated from Brambati et al. (1977))

conditions (prescribed flux) for the hydrodynamic and the morphodynamic model in the opposite side with respect to the inlet (Fig. 5.1). The Dirichlet conditions were calculated by hypothesizing that the dykes translated the actual boundary of the system to a littoral in corrispondence of the 8 m isobath: the suspended concentration was then computed as the equilibrium concentration for sea waves with a bottom composed as indicated in Tab. 3.1. Four simulations were performed and compared with different values of sediment riverine input and different subsidence rates (Tab. 3.3). In order to highlight the relevance of dealing with graded sediments, a further simulation was carried out with a unigranular sediment and compared to Sim. 1, which is the simplest in terms of sediment characterization and therefore more likely to be approximated with a unigranular system. In fact this is the case in which the mixture composition is only controlled by the sea, which is therefore the only source of sediments to be described, and in equilibrium conditions no net flux takes place giving rise to sediment selection.

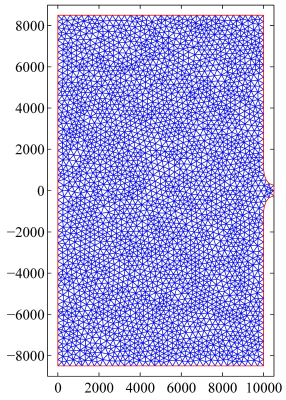

Figure 3.3: Domain discretization

class:	**1**	**2**	**3**	**4**	**5**
d_i (μm)	15.6	31.3	62.5	125	250
$Q_{s,i}$ (m^3/s)	6.35e-3	9.5e-4	4.9e-4	3.25e-3	4.29e-3
$C_{i,INLET}$ (ppm)	7.85	7.65	8.68	4.00	0.31
β_i	0.15	0.15	0.15	0.40	0.15
f_i^{tc}	4.66e-5	2.25e-5	1.12e-5	5.59e-6	2.80e-6
f_i^s	3.55e-2	1.71e-2	8.55e-3	4.26e-3	2.13e-3

Table 3.2: Model settings (Riverine sediment input, when present, boundary conditions, and initial bottom composition) and stirring coefficients. Note that the value reported here for f_i^s is only relative to the littoral, while it is set to zero inside the domain

The equivalent diameter d_0 has been chosen by imposing:

$$C_{LIM} = \frac{1}{d_0}\left(\frac{f^s}{h_{LIM}^3}\right) \tag{3.15}$$

The concentration at the inlet has been taken as the total suspended concentration, namely 28.5 ppm.

Sim.	1	2	3	4
Q_s (m^3/s)	0.00	0.00	1.24e-2	1.24e-2
Q_w (m^3/s)	0.00	0.00	65.00	65.00
α_s (mm/y)	0.00	1.00	0.00	1.00

Table 3.3: Synoptic table of the simulations performed; solid and water discharge (Q_s and Q_w respectively), and subsidence rate α_s

3.7 Results and Discussion

Before showing the results of the simulations some general considerations appear worth to be done. As a first thing, we remark that the calibration of the stirring coefficients for sea waves, as it has been carried out, represents a sort of simple submodel which allows to calculate the boundary conditions for a tidal system with no need for a detailed modelling of the complex dynamics taking place in the littoral. This property has also been used by Bonaldo and Di Silvio (2011b) with significant results.

Under the hypotheses made, spatial variations in bottom composition β_i require having a spatially variable C_i: which is impossible, in a purely dispersive system, in absence of net fluxes. On the other hand, when a factor leading to net horizontal flux is present (e.g. a river mouth, or a generalized subsidence of the basin), there will be a spatial selection based on the lag transport of the coarser sediments, thus determining a horizontal granulometric gradient in bottom composition (Van Ledden et al., 2004b).

From the analysis of the results, another factor of sediment segregation can be highlighted (Fig. 3.5), namely the entrapment on the marshes of sediments with different grainsize compared to the material in the adjacent shoals and channels. This is due to the fact that sediment deposition on the marshes is strongly enhanced by the presence of alophile vegetation, eventually setting to zero the value of the equilibrium concentration. If we consider Eq. 4.4 in morphodynamic equilibrium (vanishing time derivatives) we

notice that, while the bottom composition in absence of vegetation is controlled by both actual and equilibrium concentration, in presence of a completely developed vegetation cover the bottom composition is only controlled by actual suspended concentration and vertical exchange rate $w_{s,i}$:

$$\beta_i = \frac{w_{s,i} C_i}{\sum_j w_{s,j} C_j} \tag{3.16}$$

Hence, suspended concentration being equal for each class, the marshes will be richer in coarser sediments with respect to nearby channels and shoals. Nevertheless, being channel and shoals sediment sources for marshes, sediment selection will take place through the marsh itself, with bottom becoming progressively finer while moving towards the interior.

Concerning the morphodynamic processes (Figg. 3.4, 3.6) we find a substantial confirmation of tendencies already found in the previous work with uniform grain size (Di Silvio et al., 2010): sediment supply from rivers increases the infilling of the basin, with the formation of wider marshes with respect to the case of purely marine genesis, while both subsidence and sea level rise oppose the infilling tendency, eventually triggering the transition from a tidal lagoon to a deep bay (Sim. 2). It is worth to point out that the mesh dimension affects the minimum size of the channels, hence a systematic evaluation of the effect of the mesh size on the channel network structure would be an appropriate further step. The unigranular simulation, carried out in the same conditions as Sim. 1, resulted notwithstanding in a rather different equilibrium configuration (Fig. 3.8): the bottom is generally deeper (average depth is 0.37 m, vs. 0.26 m in the multigranular situation) and the relative surface occupied by the salt marshes is sinificantly smaller (3.4 % vs. 7.5%). This is possibly due to the lack of the bottom armouring effect acted by the coarser fraction.

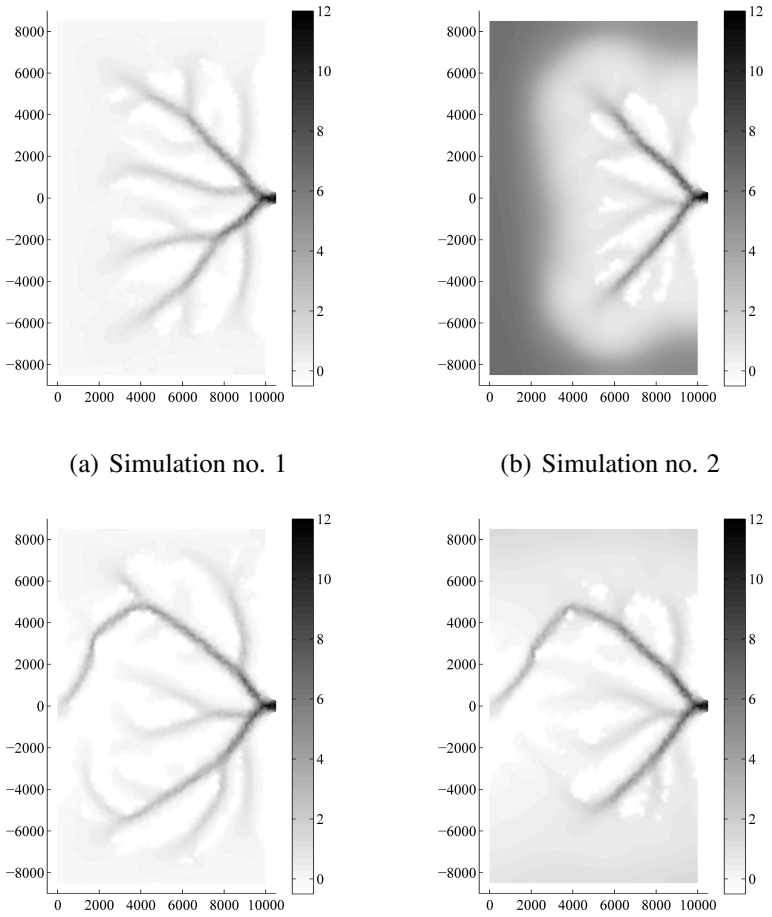

(a) Simulation no. 1

(b) Simulation no. 2

(c) Simulation no. 3

(d) Simulation no. 4

Figure 3.4: Bathymetries (m) after 6000 years

3.8 Conclusions

The multi-granular extension of a long-term two-dimensional model, based on the concepts of Tidal Dispersion and Transport Concentration is presented. This formulation allows a computationally efficient representation of sediment fluxes and morphodynamic processes at the time scale of decades to centuries, and eventually to millennia (necessary time to reach equilibrium conditions).

The mere sediment resuspension by sea waves expressed by the stirring coefficient f^s

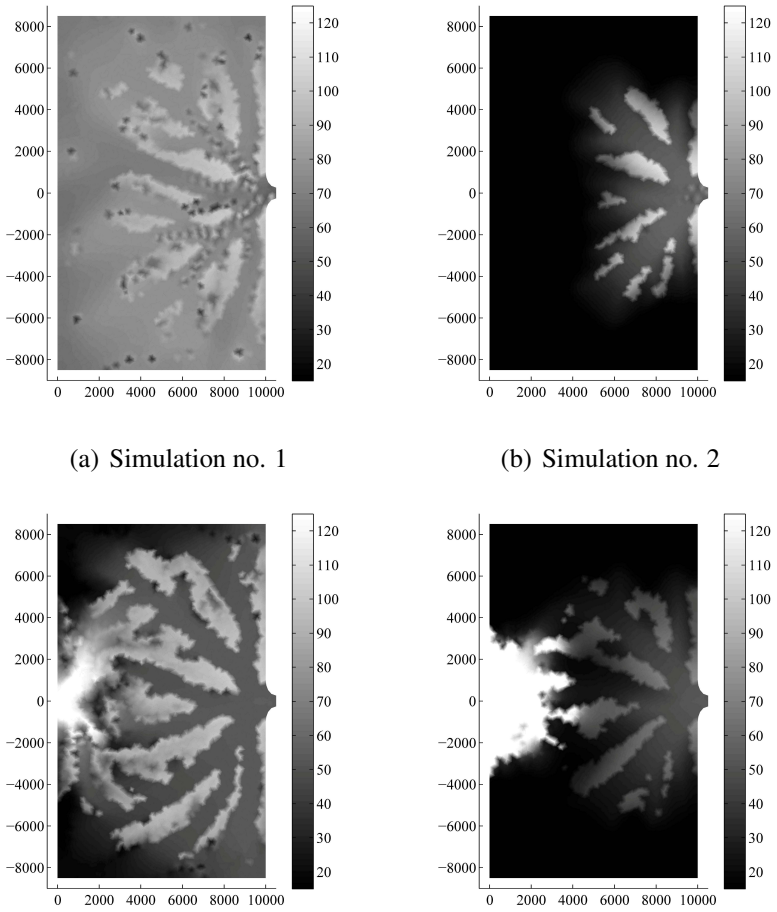

(a) Simulation no. 1

(b) Simulation no. 2

(c) Simulation no. 3

(d) Simulation no. 4

Figure 3.5: Median diameter (μm) after 6000 years

represents a very simple submodel for the computation of suspended sediment concentration profiles along cross-shore transect which makes possible to estimate the boundary conditions for a model of a tidal lagoon with no need for a detailed description of sediment fluxes in the neighbouring littoral. Indeed, the combined effects of tidal currents and sea waves within the inlet have proved to give here a plausible estimate of the concentration.

The conceptualization provided by the model gives reason of some phenomena of sedi-

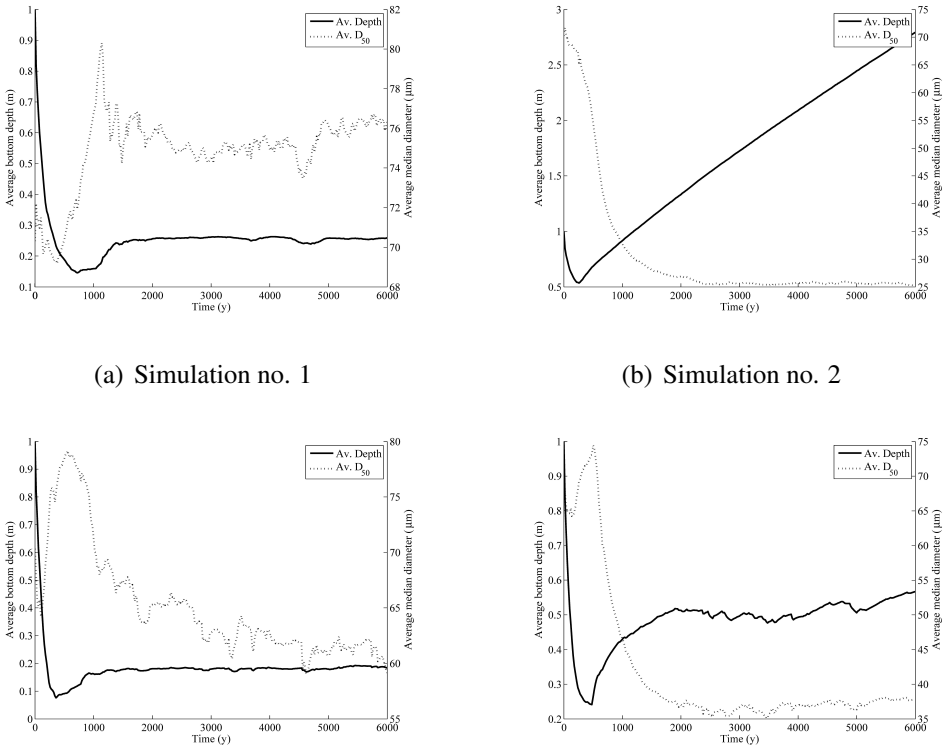

(a) Simulation no. 1

(b) Simulation no. 2

(c) Simulation no. 3

(d) Simulation no. 4

Figure 3.6: Time evolution of space averaged bottom depth and mean diameter

ment segregation in tidal basins, allowing some general equilibrium considerations and showing that this can take place both as a consequence of transport lag of coarser sediments or because of the entrapment acted by salt marsh vegetation. It is thus confirmed that horizontal transport is always necessary to create a sediment segregation, the sign of the spatial gradient invariably corresponding to a progressive fining in the flux direction (Bonaldo et al., 2010).

It has also been shown that multigranular representation of transport phenomena can be necessary even in very simple configurations, particularly if the mixture is graded enough to allow a significant difference between bottom and suspended sediment composition.

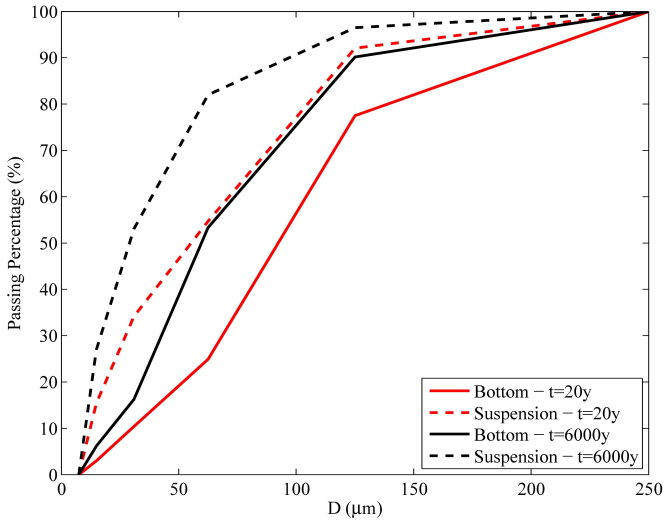

Figure 3.7: Granulometric curves for bottom and suspended sediments close to the inlet after 20 and 6000 years, Sim. 1

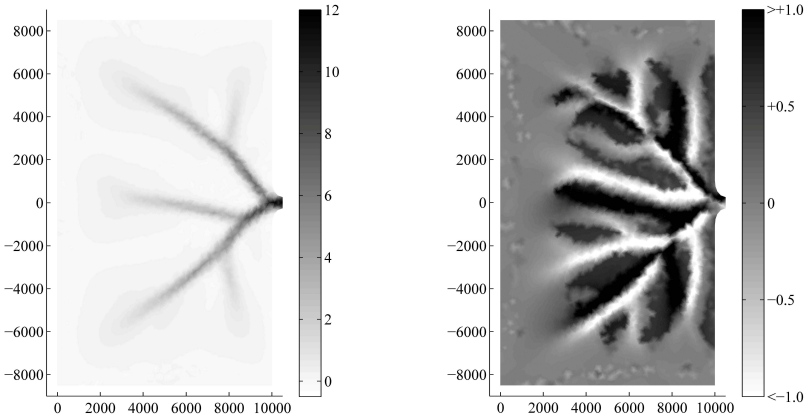

(a) Equilibrium bottom depth

(b) Depth difference between Unigranular and Multigranular

Figure 3.8: Unigranular version of Sim. 1: equilibrium bottom depth and bathymetric comparison (m)

A first application of the model is the investigation of the effects of geological and anthropogenic processes in defining the morphological and granulometric configuration of a tidal basin at the historical time scale (Bonaldo and Di Silvio, 2011b). Further developments consist in the inclusion of a schematic representation of the main sediment transport phenomena in coastal environments: this would make the model suitable for dealing with landscape genesis and evolution processes less controlled by tidal dispersion.

Chapter 4

Historical evolution of a micro-tidal lagoon simulated by a 2-D schematic model

4.1 Introduction

4.1.1 Overview

The goal of the present work is to reproduce the effects of natural and anthropogenic processes on sediment dynamics, which historically occurred during several centuries in a tidal lagoon (Lagoon of Venice in particular) by using a schematic two-dimensional morphodynamic model. The model is based on the concepts of *Tidal Dispersion*, *Net Transport* and *Equilibrium Concentration* whose early formulation was presented by Di Silvio et al. (2010) and which was recently generalized to the case of multi-granular sediments (Bonaldo and Di Silvio, 2011a) with granular behaviour (Van Ledden et al., 2004a).

The paper is subdivided as follows: in the present Section the history of the lagoon

of Venice is briefly summarized (4.1.2) as a case study of natural- and human-driven documented changes (D'Alpaos, 2010a; Favero and Serandrei Barbero, 1980; Zendrini, 1811) in order to provide a qualitative comparative term for our numerical analysis; then a short outline of the mathematical model is given (4.1.3). In Sec. 4.2 the domain geometry and the conceptual representations of each historical process are presented, while the results of the simulations are shown and discussed in Sec. 4.3. The conclusions in Sec. 4.4 point out the relevance of the work and discuss the open issues and possible further developments.

4.1.2 Geological and anthropogenic processes in tidal lagoons: the case of Venice

The lagoon of Venice, as well as other lagoons in the northern Adriatic Sea such as Caorle and Marano started its formation about 6.0-4.5 ka B.P., during the Holocene marine highstand (Fontana et al., 2008; Serandrei Barbero et al., 2001; Favero and Serandrei Barbero, 1980). After the maximum ingression (6.0 ka B.P.), a reverse in the coast movemement has been recorded due to the decrease in water supply from melting glaciers and to the considerable amount of sediments delivered by the rivers during the Atlantic period. During the subsequent period of relative stability of the coastline the first lagoonal systems started to develop behind the dune barrier, under the joint effect of soil compaction and sediment supply from rivers (with remarkable spatial variability on the significance of such sedimentary activity) (Favero and Serandrei Barbero, 1980). From 4.5 ka B.P. to 2.5 ka B.P. the littoral barrier slightly moved seawards until reaching the actual position, although with a different inlet configuration, and no significant changes in overall morphology are likely to have occurred until the sixth century a.D., when a massive flooding (*rotta della Cucca*) strongly unsettled the hydraulic configuration of the rivers flowing into the northern Adriatic Sea. The new Venice Republic was established around the beginning of the Millennium, following the invasions of the

Roman Empire by populations coming from Eastern Europe. Very soon the Republic started to operate on the rivers flowing inside the lagoon, especially the Brenta: major interventions, mainly oriented to the preservation of the lagoon from excessive infilling and the mainland from flooding and unhealthiness, began in the fourteenth century a.D. and consisted in subsequent diversions of part of the Brenta discharge, previously flowing into the central basin (Malamocco), until its complete exclusion from the central lagoon, which was completed in the early seventeenth century with the excavation of the *Taglio Nuovissimo* (Zendrini, 1811). Although the first quantitative bathimetric survey of the Venice lagoon dates back to 1811, qualitative evaluations based on previous maps (D'Alpaos, 2010a) allow to guess that, after the diversion of riverine water and sediments, the lagoon began a transition towards a different morphological conditions: namely a sensible reduction or even an inversion of the basin infilling, which was precisely the reason why the diversions were made.

At the beginning of the 19th century, following a period of negligible anthropogenic actions, the configuration of the Lagoon of Venice, represented by the Denaix's bathimetric survey, is probably close to equilibrium. After a short time, however, interventions start again: the narrowing of the lagoon inlets by means of jetties was gradually carried out (Malamocco inlet, 1820-1872; San Nicoló inlet, 1884-1897; Chioggia inlet, 1911-1933): this generated the double effect of introducing a significant asymmetry in the flow field (Blondeaux et al., 1982), with a consequent net loss of sediments from the basin (Tambroni and Seminara, 2006; D'Alpaos, 2010b), and translating the outer end of the lagoon to larger sea depths characterized by lower sediment concentration.

In the early decades of the 20th century, agricultural and industrial development policies led to land reclamations and to the excavation of the Vittorio Emanuele III Channel, linking Venice to the industrial zone of Marghera. In the second half of the century, the excavation of the Malamocco-Marghera Channel across the Central Lagoon increased the erosional trend especially of this area; moreover, the pumping of massive amounts

of water for industrial use from the aquifers brought to an enhanced subsidence of 12 cm in the 1950-1970 period.

These interventions have been qualitatively reproduced with reference to a schematic basin, as will be shown further on, and their implications will be discussed in Sec. 4.3.

4.1.3 The multi-granular Intertidal Model

The Intertidal Model as presented in Di Silvio et al. (2010) and its multi-granular extension (Bonaldo and Di Silvio, 2011a) are based on the representation of the long-term transport of sediments as a result of a tidal dispersion effect (Schijf and Schönfeld, 1953; Okubo, 1973; Dronkers, 1978) plus a net convective contribution provided by eulerian residual velocities. In the present work, nevertheless, convective contributions will not be considered: in fact, the outer littoral where convective flow is prevailing is not included in the computational domain, and the transport effect due to fluvial currents within the lagoon is normally negligible compared to tidal fluxes. The tidal dispersion is controlled by a diagonal tensor $\mathbf{D}$ whose terms are proportional to the square power of the $x-$ and $y-$ components of the velocity field in maximum flood conditions and whose order of magnitude is about 100-1000 m^2/s (Di Silvio and Fiorillo, 1981; Wang et al., 2007; Tonetto, 2009). The flow field is calculated in a simplified way (Rinaldo et al., 1999) by a devoted hydrodynamic submodel based on a simplified version of the 2-D Shallow Water Equations in which the inertial terms are neglected (Di Silvio et al., 2010; Bonaldo et al., 2010).

Net deposition and erosion are controlled (eventually for each sediment class) by the difference between the *transport* concentration, namely the long-term averaged concentration, and the *equilibrium* concentration, which represents the concentration associated to the local stirring factors in absence of net horizontal fluxes and in case of homogeneous bottom composition. The equilibrium concentration is treated as an additive quantity under the assumption that sediment resuspension is caused by a number of independent

driving forces (currents and waves) (Dal Monte and Di Silvio, 2004). For each driving force it is possible to obtain a simple expression for its contribution to equilibrium concentration by means of an appropriate manipulation of the Engelund-Hansen formula (ASCE, 1975); in particular, non-linearity and time variability arguments suggest to explicitate its dependency on known local quantities and lump all the uncertainties into appropriate *stirring coefficients* (Dal Monte and Di Silvio, 2004) which can be estimated from field measurements (Bonaldo and Di Silvio, 2011a). The expression for the equilibrium concentration for each $i-$th class, $C_{eq,i}$,corrected with a factor which takes into account for the increase in erodibility given by the bed slope α_{bot} compared to the repose angle ϕ, is thus given by:

$$C_{eq,i} = \left(f^{tc} \frac{q_{tc}^4}{h^5} + f^{rc} \frac{q_{rc}^4}{h^5} + \frac{f^s}{h^3} + \frac{f^w}{h} \right) \frac{d_i^{-1}}{1 - \frac{\tan \alpha_{bot}}{\tan \phi}} \tag{4.1}$$

where d_i is the grainsize of the $i-$th class, h is the effective depth, f_i^{tc}, f_i^{rc}, f_i^s and f_i^w are the stirring coefficients for tidal and residual currents, sea waves and internal wind waves respectively, while q_{tc} and q_{rc} are the specific discharges for tidal and residual currents respectively. A quantification of the stirring coefficients in the inlet is provided in (Bonaldo and Di Silvio, 2011a). The equilibrium concentration value in the salt marshes is corrected, and eventually set to zero, by taking into account for the trapping effect of the vegetation cover. Vegetation growth can take place when altimetric ($h < 0$) and geotechnical ($\Delta h < \Delta h_{max}$) requirements are fulfilled: any time these conditions are missing, the demolishing effect of waves can normally act.

Similarly to what has been shown in Di Silvio et al. (2010), the transport equation for each class in absence of advection can then be obtained by performing a mass budget within the water column, thus giving:

$$-div\left(\mathbf{D}h\nabla C_i\right) = w_{s,i}\left(\beta_i C_{eq,i} - C_i\right) \tag{4.2}$$

where $w_{s,i}$ is the vertical exchange coefficient, proportional to the particle diameter (Armanini and Di Silvio, 1988). The bathymetric change is the sum of subsidence and

eustatism rates (α_s and α_e) and the net erosion E, given in its turn by the sum of the net erosion for each class, namely the right-hand term in Eq. 4.2. Hence:

$$\frac{\partial h}{\partial t} = \alpha_s + \alpha_e + \sum_i E_i \tag{4.3}$$

A further sediment budget is required in the mixing layer, beside the one performed in the water column, to describe the time variation in the bottom composition (Di Silvio and Padovan, 1998):

$$\frac{\partial (\beta_i \delta)}{\partial t} = -E_i + \beta_i^* E \tag{4.4}$$

β_i^* represents the fraction of $i-$th class in the origin of the vertical fluxes, which can be either the mixing layer or the underlying zone, depending on the fact that a net deposition or erosion is taking place. The thickness of the mixing layer δ has been assumed, as a first approximation, spatially uniform and equal to 0.20 m.

4.2 Model setup

The computational domain is a rectangular basin, as represented in Fig. 4.1, with a surface of (17x10) km^2, more or less corresponding to the Malamocco basin of the lagoon of Venice. The domain has been discretized with a triangular mesh with a characteristic dimension of about 250 to 300 metres; the boundaries are supposed to be impermeable with the exception of the inlet, where Dirichlet conditions have been imposed, and of the river mouth, flowing into the north-western end of the basin during the genesis of the lagoon and then diverted outside the domain. In order to reproduce the segregation of sediments with different grain size within the basin (Barillari, 1977-78, 1980-81), and to study selective sediment fluxes through the inlet under different inlet configurations, in the present work two different grain classes have been considered, which will be identified from now on as d_1 (31 μm) and d_2 (125 μm). These classes lump all the grain sizes respectively finer and coarser than 62 μm and have been chosen in order to have

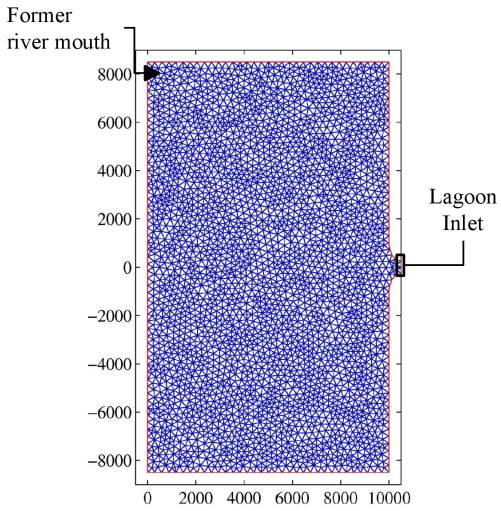

Figure 4.1: Model domain

the same order of magnitude in terms of relative presence on the littoral and inside the lagoon (Brambati et al., 1977). Both classes are supposed to have granular behaviour: this does not imply that cohesive material is absent at all, but simply that the sand content of the mixture is high enough to control its behaviour (Van Ledden et al., 2004a). After the genesis of a tidal channel network in the basin and the attainment of an equilibrium lagoon under the combined stirring effect of sea and internal wind waves, tidal and fluvial currents, riverine sediment input, tidal dispersive transport, subsidence and sea level rise; the model has been subject to four different evolutions, each one 600 years long, by changing in sequence some of the forcing factors as historically occurred:

1. river Brenta diversion from Malamocco basin at a. D. 1600, then undisturbed evolution.

2. river diversion, jetties construction after 250 years (a. D. 1850).

3. river diversion, jetties construction after 250 years and increased subsidence between years 350 and 370 (from a. D. 1950 to 1970).

4. river diversion, jetties construction after 250 years, increased subsidence from 350 to 370, and regular dredging of an artificial channel starting from year 365 (a. D. 1965).

In the following some details are reported about the relevant conditions and forcing factors.

4.2.1 Genesis of the tidal lagoon

The lagoon has been generated starting from a flat bottom basin situated 0.5 m below the mean sea level and with a uniform initial composition with an equal ripartition between the two sediment classes. The inlet width was assumed equal to 1000 m, as shown for Porto di Malamocco in the old maps, before the jetties construction. The stirring coefficients for the only resuspension mechanisms acting on the inlet (sea waves and tidal currents), namely f^{tc} and f^{s} in Eq. 5.1, have been calibrated as explained in Bonaldo and Di Silvio (2011a); note that the value of f^{s} is equal to the calibration one just on the outer boundary of the inlet, and it has been assumed to be linearly decreasing to zero within 1 km inward of the boundary cross-section. For simulating the increasing effect of the fetch length of the dominant local wind (Bora) along the Malamocco basin, the stirring coefficient for internal waves f^{w} has been assumed linearly increasing in the SouthWest direction from 1.75E-07 to 1.75E-6 m. These values have euristically been chosen in order to provide a realistic bottom depth on the shoals.

The concentration at the inlet for each class has been chosen equal to the equilibrium concentration in the littoral at the minimum depth of the external delta, namely 4 metres below the mean sea level, as reasoned by Bonaldo and Di Silvio (2011a). The amplitude of the reference tidal wave is 0.35 m; the time-averaged sediment discharge flowing from the river has been assumed equal to 0.50 m^3/s, very likely quite larger than the Brenta river transport in the present conditions. The distribution of the transport

between the finer and the coarser fraction has been estimated on the basis of a realistic bottom composition in the lower reach of the river. The corresponding water flow (115 m^3/s) is only relevant in terms of sediment resuspension: close to the mouth, but not in terms of net transport, which is totally dominated by the (inter) tidal dispersion. The rates of subsidence and sea level rise were assumed equal to 1.33 mm/y and 0.33 mm/y respectively (Brancolini et al., 2006). The boundary conditions are summarized in Table 4.1.

Class	C_{INLET} (-)	$Q_{s,i}$ (m^3/s)
1	1.34E-05	4.50E-01
2	3.50E-05	5.00E-02

Table 4.1: Lagoon genesis: concentration at the inlet and riverine input

4.2.2 River diversion

The diversion of the river has been made instantaneously after an equilibrium condition for the lagoon was attained. This operation was simply modeled by imposing nil fluxes through the nodes previously representing the river mouth.

4.2.3 Jetties construction

The contruction of the jetties was simulated by a variation of the geometry and of the boundary conditions. In terms of geometry, the width of the inlet was reduced to 500 m, while in terms of suspended concentration the hypothesis was made that the sheltering effect performed by the jetties was such that the sediment resuspension produced by the sea waves was negligible also in the inlet. In this way, the equilibrium concentration expressed by Eq. 5.1 is only dependent on the tidal currents. As shown again by Bonaldo and Di Silvio (2011a), these two conditions provide the new value of the concentration

for the different classes (C_1 =1.98E-05, C_2 =8.56E-06), together with a deepening of the channel and a coarsening of the bed.

4.2.4 Human-induced soil compaction

The increase of soil compaction related to the pumping of excessive volumes of groundwater in the period 1950-1970 was represented by adding to the natural subsidence rate a further contribution of 6 mm/y.

4.2.5 Channel dredging

The excavation (in 1963) and the subsequent maintenance of the navigation channel crossing the upper half of the basin, was modeled as a permanent modification of the depth of the channel, imposed greater or equal to 15 m. The amount of sediments deposited on the channel bottom, recorded at every iteration, provides the necessary information about the trapping effect acted by the channel.

4.3 Results and Discussion

4.3.1 Genesis of the tidal lagoon

The infilling of the basin by both sea and river generated a lagoon very rich in salt marshes and characterized by a significant spatial variability of bottom composition. As pointed out by Bonaldo and Di Silvio (2011a), two factors of sediment segregation have been operating: on one hand the distance from the source (the river delivered finer sediments than the sea), and on the other hand the tendency of salt marshes to be preferentially fed with the coarser fraction of the surrounding suspended material.

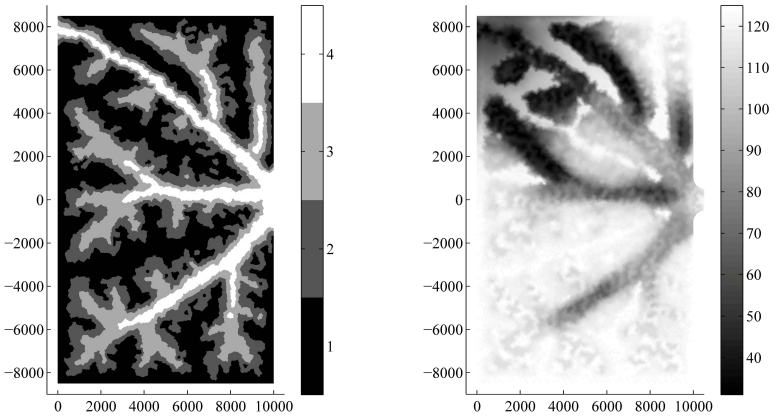

(a) Bottom morphology (b) Mean diameter (μm)

Figure 4.2: Initial configuration. Morphological features are represented as: 1: vegetated marshes; 2: upper intertidal (h =-0.35 to 0 m); 3: shoals (h =0 to 1 m); 4: channels (h >1 m)

4.3.2 River diversion

Immediately after the diversion of the river (which in reality was a rather gradual operation) there is a sudden loss of a significant salt marsh area (Fig. 4.8). The average grain size initially increases, since the important source of fine sediments represented by the river is now absent, but after about 100 years the trend gradually reverses as the subsidence enhances the deepening of the bottom and its consequent, although very slight, refinement (Bonaldo and Di Silvio, 2011a). The maximum depth at the inlet displays a very small (because of the large exponent of h in the expression of f^c) initial decrease, due to the dominant effect here of the tidal currents and to the lack of the river current acting as a stirring factor.

250 years after the river diversion (Fig. 4.3) the sediments have been redistributed within the basin, with a spatial, subsidence-driven, fining from the inlet towards the interior of the basin, and a residual zone of finer material in the vicinity of the former river mouth; almost all the marshes originally distributed along the inner boundary of the lagoon dis-

appear due to the dominance of the subsidence on the sediment supply from the sea. After 600 years (Figg. 4.5, 4.6 and 4.7) these results are more marked, but the evolutionary trend is rather slow.

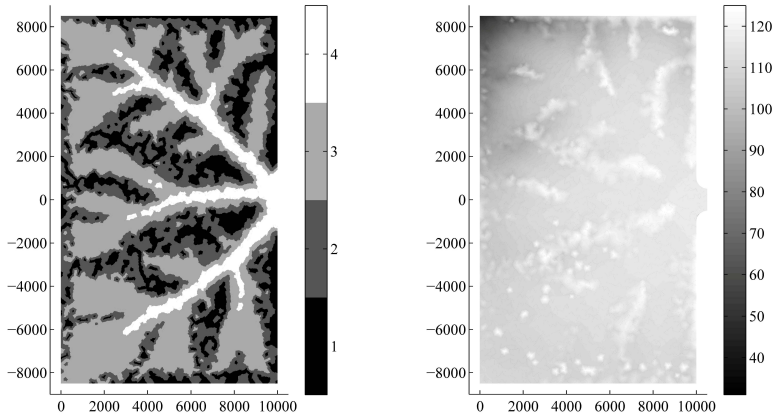

(a) Bottom morphology (b) Mean diameter (μm)

Figure 4.3: Configuration 250 years after the river diversion. Morphological features are represented as: 1: vegetated marshes; 2: upper intertidal; 3: shoals; 4: channels

4.3.3 Jetties construction

When the jetties are built, the immediate result is a prompt response of the inlet bottom depth to the new geometric constraints (Fig. 4.8), which generates a temporary intense seaward flux of the sediments moved during this process (Fig. 4.9). The permanent reduction of sediment concentration at the boundary, moreover, sustains an increased overall outward flux. On the other hand, the contextual increase of finer sediments at the boundary causes an increase of the inflowing fluxes of finer sediment, while the coarse fraction undergoes a reverse in the fluxes for the first decades until a parlty recovering of the previous trend of net sediment import from the sea. Thus, the average grain size within the basin rapidly decreases, while the reduction in the overall sediment

availability from the sea enhances the gap between subsidence (and sea level rise) and sediment supply from the sea, inducing a generalized deepening of the basin (Fig. 4.7) and a faster loss of vegetated marshes.

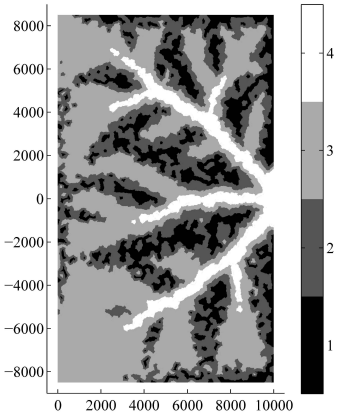

(a) Bottom morphology, no jetties

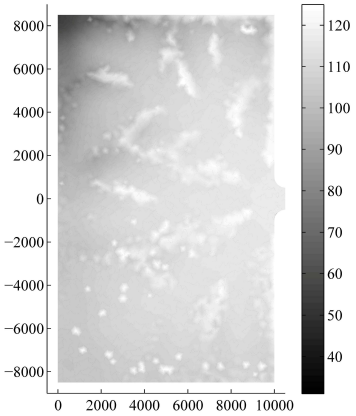

(b) Mean diameter (μm), no jetties

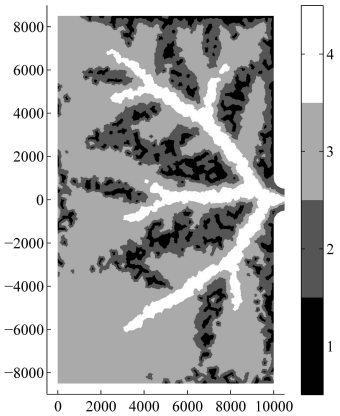

(c) Bottom morphology 100 years after jetties construction

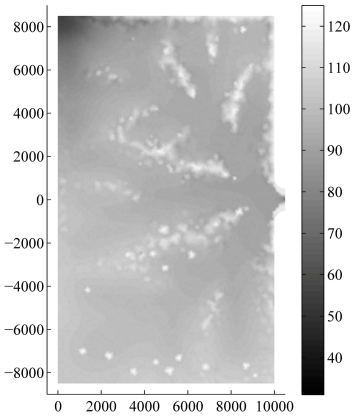

(d) Mean diameter (μm) 100 years after jetties construction

Figure 4.4: Configuration 350 years after the river diversion, with and without jetties. Morphological features are represented as: 1: vegetated marshes; 2: upper intertidal; 3: shoals; 4: channels

4.3.4 Human-induced soil compaction

A strong increase in the subsidence rate has substantially the effect of increasing, to different extents, the processes ongoing in the system. In particular, the average bottom composition and the inlet geometry are minorly affected by subsidence, while bottom depth and consequently the alophile vegetation cover undergo an important modification (Fig. 4.8).

4.3.5 Artificial channel dredging

Figg. 4.6, 4.7 and 4.8 show that the morphological degradation process of the lagoon is hugely increased by the excavation of the artificial channel. The dramatic morphological impacts of the channel are spatially described in Fig. 4.10, which represents the depth differences between Evolution 4 and 3 at the end of the simulations: it can be seen that the entire channel network acts now as a sediment trap to the detriment of the adjacent shoals. The presence of a deep channel far from its equilibrium condition induces a net flux of sediments from the sea (Fig. 4.9) and the shoals: such a flux gives rise to a spatial selection of sediments (Bonaldo and Di Silvio, 2011a), with a resulting grainsize coarser in the vicinity of the sources and finer on the channel.

A granulometric gradient is generally present in the inlet, with a fining trend toward the interior of the basin (Molinaroli et al., 2007; Ferrarin et al., 2010), where the grainsize distribution is determined by the fluxes given by subsidence, changes in boundary conditions and sediment trapping by channel dredging.

The decrease in salt marshes surface takes place as an effect of generalized sinking, erosion by waves (Favero and Serandrei Barbero, 1980; Carniello et al., 2009) and, to a lesser degree, to particular flow conditions associated to the tidal currents: in equilibrium conditions these factors are generally contrasted by the sediment trapping acted by alophile vegetation, provided that the sediment supply is rich enough to contrast the ero-

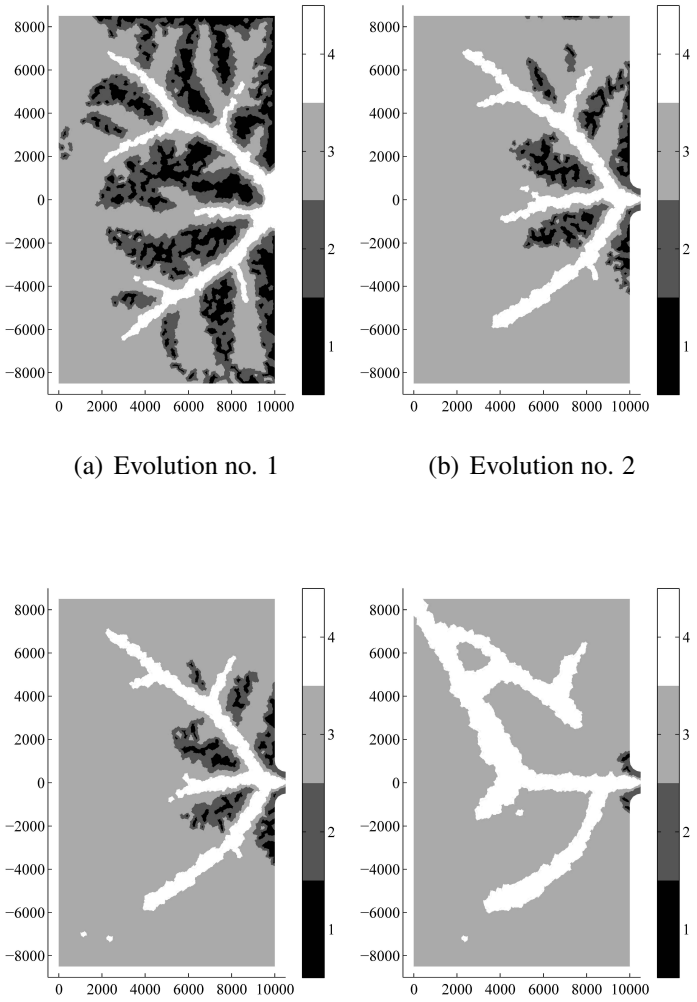

(a) Evolution no. 1 (b) Evolution no. 2

(c) Evolution no. 3 (d) Evolution no. 4

Figure 4.5: Final morphological configurations, 600 years after river diversion. Morphological features are represented as: 1: vegetated marshes; 2: upper intertidal; 3: shoals; 4: channels

sion acted by waves and to keep pace with subsidence and sea level rise. A modification in one of these factors leads to a different equilibrium configuration of the salt marsh pattern; nevertheless the presence of vegetation improves the resilience of the marshes and, to some extent, of the whole tidal system. Indeed, besides preventing the marsh

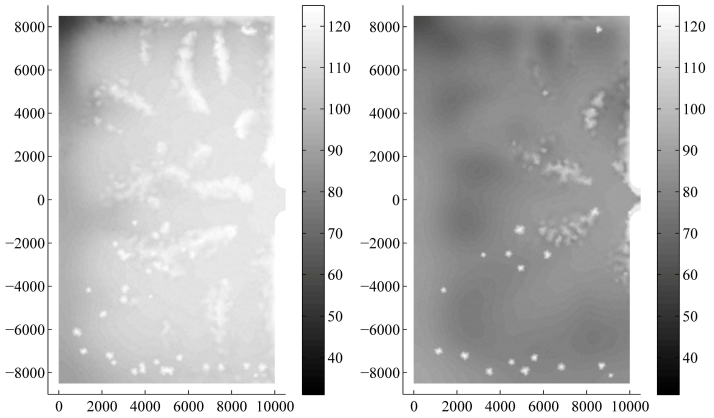

(a) Evolution no. 1 (b) Evolution no. 2

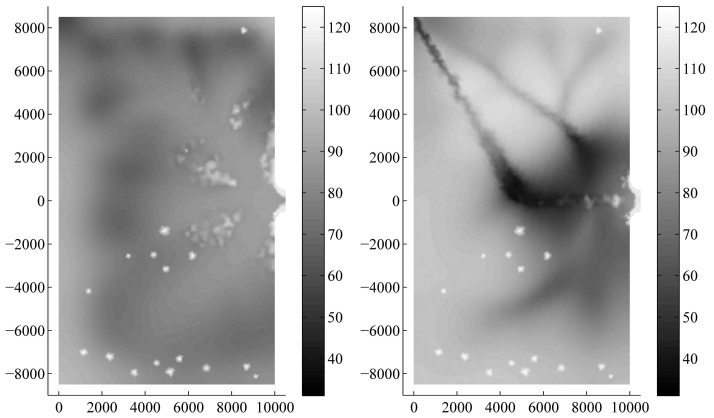

(c) Evolution no. 3 (d) Evolution no. 4

Figure 4.6: Final mean diameters (μm), 600 years after river diversion

bottom from erosion, in case of a generalized loss of sediments from the basin, alophile vegetation is able to feed the marshes with part of the sediments eroded from the shoals (or even from collapsed neighbouring marshes) and dispersed by the tidal currents.

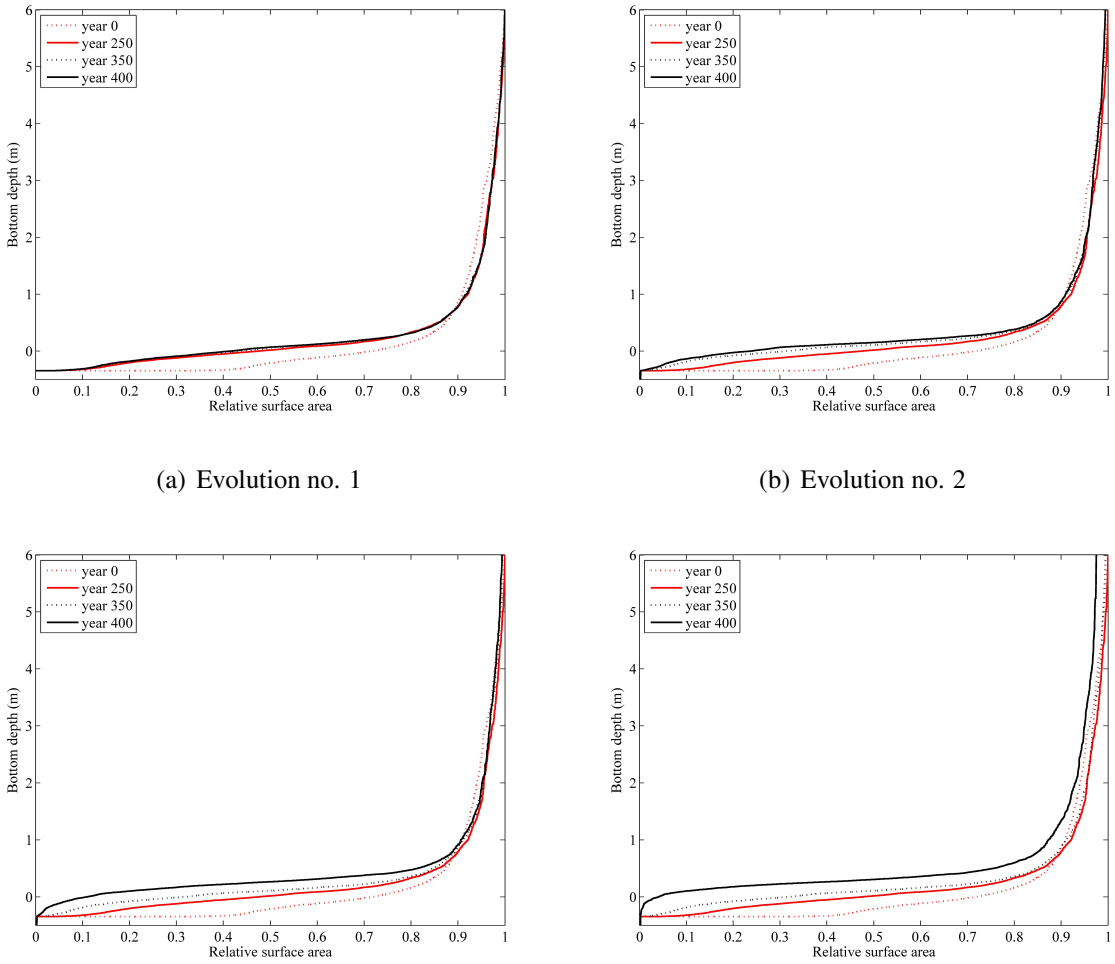

(a) Evolution no. 1

(b) Evolution no. 2

(c) Evolution no. 3

(d) Evolution no. 4

Figure 4.7: Hypsometric curves for each evolution

4.4 Conclusions

The application of a long term morphodynamic model to a schematic basin qualitatively similar, in terms of geometry, history and forcing factors, to the Malamocco basin in the lagoon of Venice, has given the opportunity of reproducing and interpreting some of the major natural and anthropogenic events which took place there in the last centuries.

The results presented in this section qualitatively agree with documented evidences (Carniello et al., 2009; D'Alpaos, 2010a; Sarretta et al., 2010). Although the the average bottom depth appears underestimated compared to the Malamocco basin of the Venice lagoon (1.75 m, according to Sarretta et al. (2010)), its trend is well reproduced by the model: as well as the Malamocco basin underwent a depth increase of nearly 270% in the period from 1927 to 2002, a very similar relative increase took place in the schematic basin (Sim. 4).

The planimetric distribution of the salt marshes is rather different from the one that can be presently found in the Malamocco basin: while in the real basin the few residual marshes are concentrated close to the internal end of the lagoon, in the schematic model they are relatively closer to the inlet: which is reasonable, being the sea the only available source of sediment. A possible explanation for this different behaviour is that, in natural systems, local wind conditions are more important than the sediment availability in determining the genesis and distribution of a marsh zone: hence introducing some simplified way to take into account for the local fetch, depending for example on the planimetric salt marsh pattern, would probably lead to some improvement in the results. Since the qualitative trends are well represented, a good quantitative agreement with the measured evidences can presumably be achieved, at least in terms of global properties, by an appropriate tuning of wind stirring coefficient and stability criterion for the salt marshes (affecting the average bottom depth and the vegetation pattern) and the value of the dispersion coefficient (influencing the velocity of the evolution). Another point that deserves some further consideration is the initial condition of the Lagoon when rivers were diverted: while in the present work the hypothesis has been made of substantial equilibrium condition, one would also consider that a slight tendency to overall silting was possibly still active.

To summarize the relative impact of the different human interventions, it can be concluded that the river diversion, though very important for the Venetian Republic (Zen-

drini, 1811), seems likely to have had a minor role in the morphological degradation of the present lagoon compared to the more recent works, whose impacts were highlighted for instance by D'Alpaos (2010b). Anyway, a vivid debate is still ongoing about the impacts of past and future interventions, whose investigation is actually the endeavour of the present work.

It is worth to point out that an important factor of net loss of sediments, namely the asimmetry of the tidal fluxes (Blondeaux et al., 1982), was here not taken into account. At a long time scale, such a net sediment transport which is not related to either a concentration gradient or a residual flow field (with a net water transport), may be considered as a *pseudo-convective* transport process, which requires, for being properly reproduced by the model, a specific conceptualization which will be the focus of some future developments. The introduction of this class of transport phenomena would significantly enhance the applicability of the model, allowing to extend the analysis also to more complex coastal systems where dispersive transport is not dominant as it is in a lagoon and where planimetric evolution plays a major role.

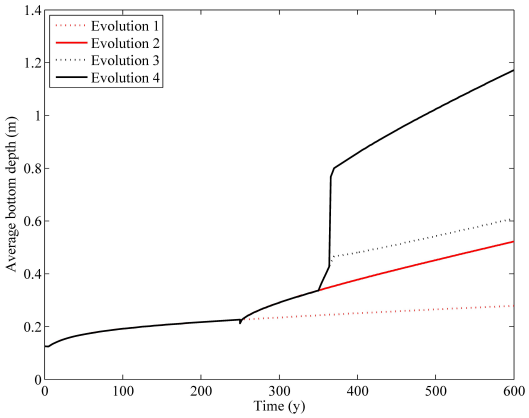

(a) Average bottom depth

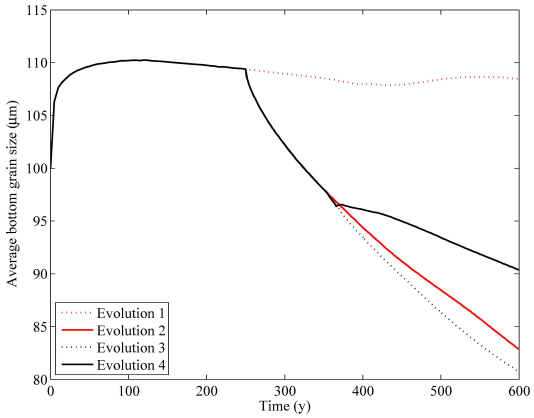

(b) Average diameter

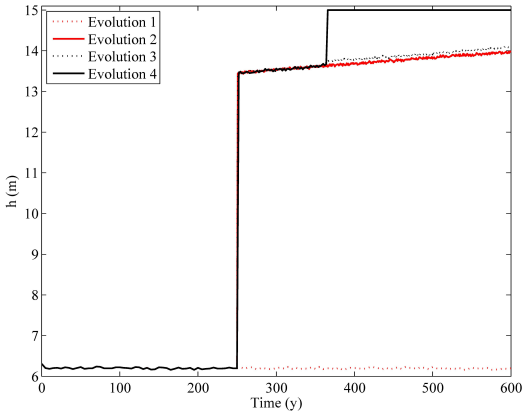

(c) Maximum depth at the inlet

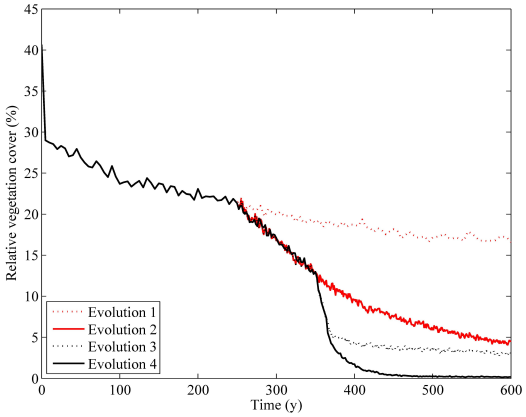

(d) Relative vegetation cover

Figure 4.8: Time evolution of some global properties

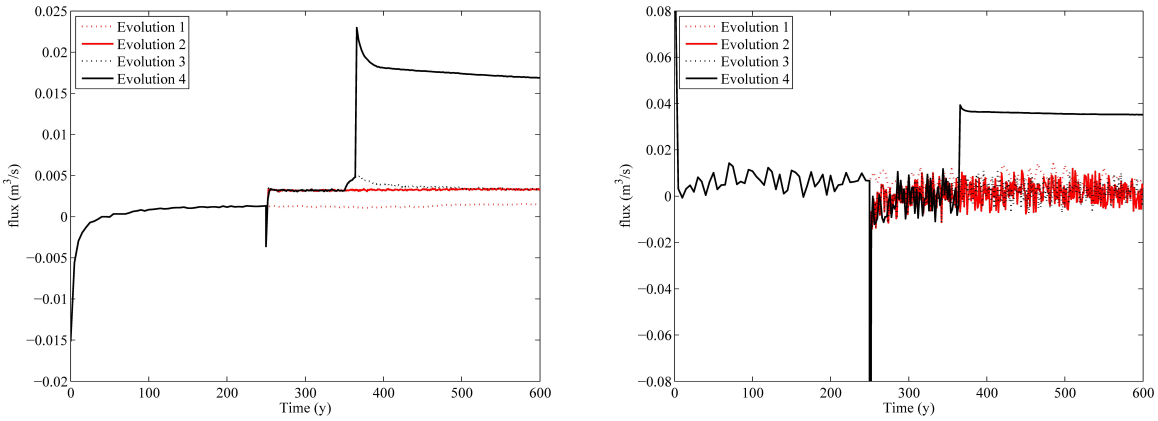

(a) Class 1 (b) Class 2

Figure 4.9: Sediment fluxes through the inlets. Oscillations in Class 2 fluxes are due to numerical noise

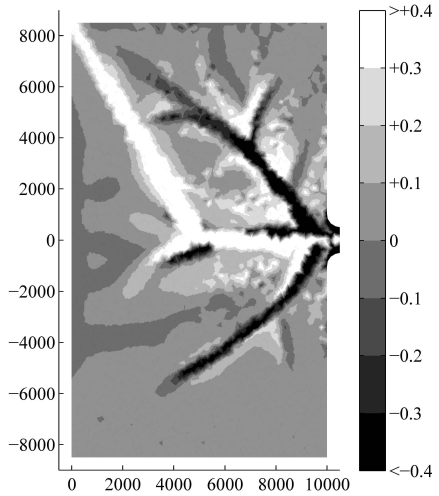

(a) Depth increase after 50 years with respect to the no-canal scenario

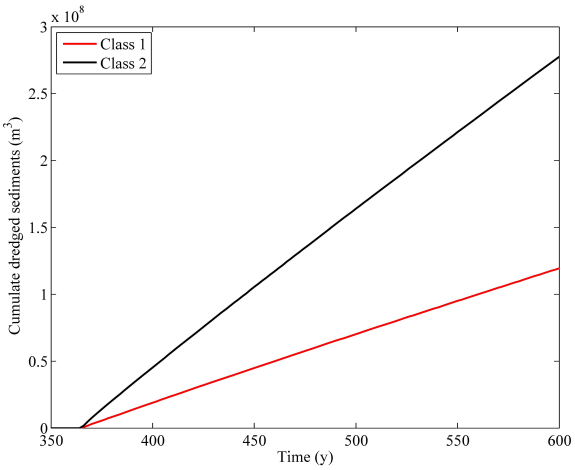

(b) Cumulative sediment trapping within the navigation canal

Figure 4.10: Impact of the excavation and maintenance of the artificial channel

Chapter 5

Morphological consequences of the nodal modulation on a tidal lagoon

5.1 Introduction

The changes in lunar declination taking place with a period of 18.6 years result in a so-called *nodal modulation* of all tidal constituents (Pugh, 1996). In particular, the most energetic semi-diurnal component M2 is subject to a modulation of about 4 % of the mean tidal range, slightly variable in time and space depending on local hydrodynamic conditions and sea level rise (Camuffo, 1993; Ray, 2006; Shaw and Tsimplis, 2010; Woodworth, 2010).

According to some Authors, the nodal modulation of the tidal range has a remarkable environmental (Yndestad et al., 2008; Yndestad, 2009) and morphological importance (Oost et al., 1993; Gratiot et al., 2008). Jeuken et al. (2003) point out that the nodal cycle is the only known hydrodynamic cycle, with such a long period, to be able to influence the tidal currents in tide-dominated estuaries and hence erosion and sedimentation processes. In fact, morphological features in estuaries and tidal lagoons are related to the tidal prism (O'Brien, 1931; Di Silvio, 1989; Dal Monte and Di Silvio, 2003; Townend,

2010) and thus an oscillation in its amplitude can eventualy lead to an alternate reversal in the sediment fluxes between the sea and the system itself: with relevant morphological effects, since the long-term morphodynamic evolution of tidal systems is usually given by small differences between great fluxes (Townend and Whitehead, 2003).
In order to provide a quantitative evaluation of the morphological effect of the nodal tide, a simplified model was previously applied by Jeuken et al. (2003) with a satisfactory agreement with experimental data collected on the Humber and Westerschelde estuaries. These studies shown that the response of a system to a nodal tidal forcing varies along the estuary depending on various parameters. The investigations performed so far focused on the behaviour of the estuary main channel. The goal of the present work is to extend the analysis to the other components of a tidal system, namely shoals and salt marshes. To this aim, a two-dimensional, vertical averaged, long-term morphodynamic model has been applied (Di Silvio et al., 2010), based on the *Tidal Dispersion* and *Equilibrium Concentration* concepts. This model has been recently improved by introducing the ability to deal with graded sediments (Bonaldo et al., 2010; Bonaldo and Di Silvio, 2011a), but we have hypothesized here uniform sediments, in order to reduce the complexity of the problem and provide a clearer picture of the sole effects of the nodal tide. The combined effect of nodal tide and steady net fluxes due to sea level rise are also investigated.

5.2 Model formulation and setup

The long-term model presented by Di Silvio et al. (2010) (from now on referred to as *Intertidal Model*) is based on the concept of *Transport Concentration*, defined as the long-term averaged sediment concentration, provided in a given location by the balance of the horizontal transport and the vertical exchanges between the water column and the bottom. The long-term horizontal transport can either be proportional to the

transport concentration (convection) or to its spatial gradient (dispersion). Closely related to the transport concentration is the concept of *Equilibrium Concentration*, namely the time-averaged concentration for which the upward flux (entrainment) is equal to the downward flux (deposition). Its quantification as a sum of various contributions is relatively straightforward if the water motion responsible for sediment entrainment is caused by independent driving forces; in this case for each driving force (currents or waves) it is possible to obtain a simple expression for its contribution by means of an appropriate manipulation of the Engelund-Hansen formula (ASCE, 1975). In particular, non-linearity and time variability arguments suggest to explicitate its dependency on known local quantities and lump all the uncertainties into appropriate *stirring coefficients* (Dal Monte and Di Silvio, 2004; Di Silvio et al., 2010) which can be estimated from field measurements (Bonaldo and Di Silvio, 2011a). In case of uni-granular sediment, the expression for the equilibrium concentration C_{eq},corrected with a factor which takes into account for the increase in erodibility given by the bed slope α_{bot} compared to the repose angle ϕ, is thus given by:

$$C_{eq} = \frac{f^{tc}\frac{q_{tc}^4}{h^5} + f^{rc}\frac{q_{rc}^4}{h^5} + \frac{f^s}{h^3} + \frac{f^w}{h}}{1 - \frac{\tan\alpha_{bot}}{\tan\phi}} \tag{5.1}$$

where h is the local effective depth, namely the bottom depth weighed with the submergence time (Di Silvio et al., 2010), f^{tc}, f^{rc}, f^s and f^w are the stirring coefficients for tidal and residual currents, sea waves and internal wind waves respectively, while q_{tc} and q_{rc} are the specific water discharges for tidal and residual currents respectively. As the effect of bathimetry is explicitly accounted for by the depth h, the stirring coeficients and the water discharges (depending only on the planimetric characteristics of the estuary) may be considered as constant values during the estuary evolution. A quantification of the stirring coefficients along the littoral and on the inlet is provided by Bonaldo and Di Silvio (2011a). Where two topographic conditions are fulfilled (bottom elevation above the mean sea level greater than zero and prominence over the neighbouring points smaller

than a geotechnical threshold value) alophile vegetation growth can occur with a simple first-order kinetic process transforming the shoal into a salt marsh: in this situation the equilibrium concentration is set to zero in order to represent the sediment trapping and bottom strenghtening effect acted by vegetation stems and roots.

As already mentioned, the horizontal transport considered by the model is the sum of a *dispersive transport*, namely the long-term effect of a number of tidal cycles integrated over time (Schijf and Schönfeld, 1953; Okubo, 1973; Dronkers, 1978), and a *convective transport*, which can be given for example by residual eulerian currents or long-shore littoral drift. However, as done in previous papers (Bonaldo et al., 2010; Bonaldo and Di Silvio, 2011a,b), we focus on a tidal lagoon without considering the outer littoral and in addition we will not consider the presence of any relevant river input, thus having no net convective transport. The tidal dispersion is controlled by a tensor **D** whose diagonal terms are proportional to the square power of the $x-$ and $y-$ components of the velocity field in maximum flood conditions.The proportionality coefficient is a calibration parameter, including the effect of all the variables which can not explicitly be taken into account, which has been estimated to have an order of magnitude of some hundreds seconds (Dal Monte and Di Silvio, 2004; Tonetto, 2009): this produces, for typical tidal velocities, values of the dispersion tensor comparable with others which can be found in literature (Di Silvio and Fiorillo, 1981; Wang et al., 2007). Under the assumption that sediment accumulation within the water column is negligible compared to the vertical fluxes to and from the bottom, a sediment balance on the water column requires that the divergence of the horizontal fluxes is equal to the net erosion of the bottom itself, namely:

$$div\mathbf{W}hC - div\left(\mathbf{D}h\nabla C\right) = w_s\left(C_{eq} - C\right) \tag{5.2}$$

C is the transport concentration, **W** is the convective residual flow (assumed negligible here) and w_s is the vertical exchange rate, proportional to the particle fall velocity (Armanini and Di Silvio, 1988). The right-hand term in Eq. 5.2 represents the net erosion

rate.

The bathymetric change is the sum of subsidence and eustatism rates (α_s and α_e) and the net erosion, hence:

$$\frac{\partial h}{\partial t} = \alpha_s + \alpha_e + w_s \left(C_{eq} - C \right) \tag{5.3}$$

The morphodynamic model is coupled with a simplified hydrodynamic submodel which computes the tidal flow field in maximum flood conditions, providing the water velocity components required to calculate the tidal contribution to C_{eq} and the dispersion tensor **D**. The hydrodynamic submodel solves, under the hypothesis of short tidal basin and instantaneous propagation of the tidal wave, a simplified version of the 2-D Shallow Water Equations in which the inertial terms are neglected: further details can be found in Di Silvio et al. (2010).

Both the hydrodynamic and morphodynamic model are solved via a Finite Element discretization of the partial differential equations describing the processes. The domain is divided into a triangular mesh and the approximated solution is given in terms of linear base functions. The computational time step is chosen in such a way to warrant the maximum difference in bottom depth in any node of the basin to be smaller or equal to a previously defined threshold.

Since our goal is to study the general behaviour of nodal tide to estuarine systems, we applied the Intertidal Model to a schematic typical microtidal basin to be conveniently adapted to other conditions. The reference model domain is a rectangular domain of 10x17 km (the surface area will be referred to as A_{ref} later on), discretized in a mesh with a characteristic dimension of about 300 m (Fig. 5.1), which will subsequently be modified in various ways in order to assess the response of the system under different driving forces. The time-averaged tidal range (about 0.70 m) and the size of the benchmark are more or less those of the present central basin of the lagoon of Venice.

Dirichlet conditions (prescribed concentration) were set at the inlet and calculated by

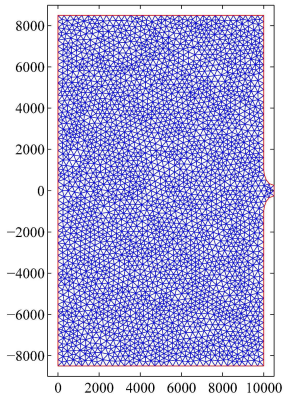

Figure 5.1: Domain discretization

hypothesizing that the jetties translate the actual boundary of the basin into the outer littoral as far as the 8 m isobath: the suspended concentration was then computed as the equilibrium concentration for sea waves at that depth (Bonaldo and Di Silvio, 2011a,b). In some simulations this computational domain was scaled by a factor 1/2 and 1/4.

As a first thing the effect of nodal tide on the equilibrium conditions (and their attainment) of the benchmark lagoon was studied. Such a lagoon, generated by the same model, is characterized by the coexistence of a channel network, tidal flats, and salt marshes and has been obtained by assuming a suspended concentration at the inlet C_{INLET} =20 ppm (Bonaldo and Di Silvio, 2011a), a constant stirring coefficient for internal wind waves f^w =1.0E-6 m and a sea level rise rate α =0.3 mm/y. No sea waves were considered in this case, based on the assumption that they dissipate most of their energy within a small distance from the outer end of the jetties. It can be argued that the value assumed for the eustatism rate is rather small, but it was chosen in order to obtain the desired equilibrium configuration also in absence of sediment supply from the rivers (although instrumental for the genesis of the lagoon of Venice, for example, whence they were mostly diverted during the XVI century).

Subsequently other equilibrium systems were created, without nodal tide, with different forcing factors or different geometries: these equilibria were then perturbed with a nodal modulation of the tidal range and some reference quantities were analized by means of a Fourier analysis. Tab. 5.1 summarizes the values of the parameters used for these simulations, respectively wind waves stirring coefficient f^w, mean tidal range η, eustatism rate α, grainsize d, and basin surface area normalized with the area of the reference geometry A/A_{ref}. Sim. 1 is the bechmark, and the others were obtained by modifying one or more parameters (highlighted in bold). Sim. 11 has the same properties as Sim. 1, included the surface area, but a different planimetric configuration characterized by a funnel shape, 60 km long and 9 km wide at the mouth. Parameters selected for the various simulations are not always mutually coherent from the physical point of view nor strictly consistent with the model's simplifications. They have been used, in fact, for a preliminary sensitivity analysis of the nodal tide effect.

Sim.	f^w (m)	η (m)	α (mm/yr)	d (μm/y)	A/A_{ref} (-)
1	1.00E-06	3.50E-01	3.00E-01	6.20E+01	1.00E+00
2	1.00E-06	3.50E-01	**6.00E-01**	6.20E+01	1.00E+00
3	1.00E-06	3.50E-01	**0.00E-00**	6.20E+01	1.00E+00
4	**4.00E-06**	3.50E-01	**-3.00E-01**	6.20E+01	1.00E+00
5	**4.00E-06**	3.50E-01	3.00E-01	6.20E+01	1.00E+00
6	**4.00E-06**	3.50E-01	**0.00E+00**	6.20E+01	1.00E+00
7	1.00E-06	**7.00E-01**	3.00E-01	6.20E+01	1.00E+00
8	1.00E-06	3.50E-01	3.00E-01	**1.25E+02**	1.00E+00
9	1.00E-06	3.50E-01	3.00E-01	6.20E+01	**2.50E-01**
10	1.00E-06	3.50E-01	3.00E-01	6.20E+01	**6.25E-02**
11	1.00E-06	3.50E-01	3.00E-01	6.20E+01	1.00E+00

Table 5.1: Simulations performed

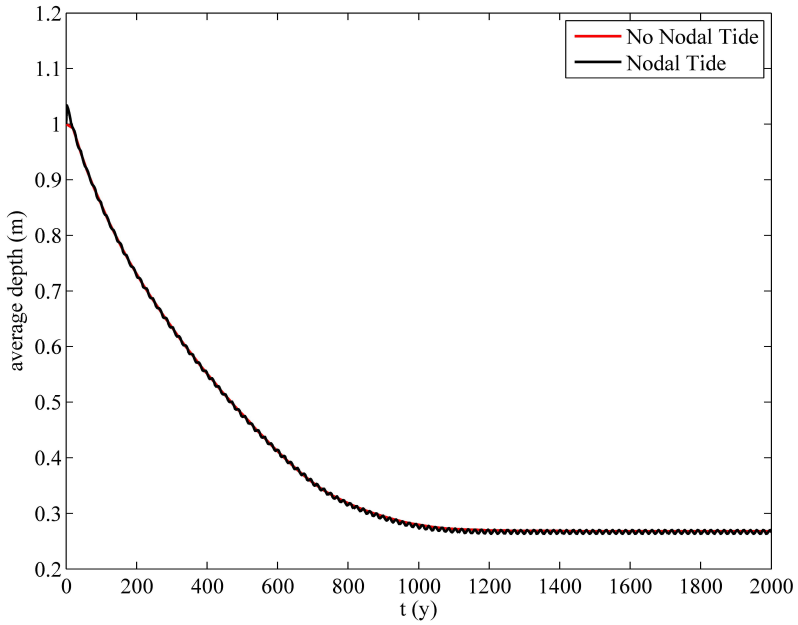

Figure 5.2: Lagoon genesis: space-averaged bottom depth

5.3 Results and Discussion

5.3.1 Equilibrium of a tidal lagoon

In order to compare the effect of the nodal tide on the genesis and development of a tidal lagoon, the average bottom depth was chosen as an overall indicator of the evolution of the system. As it can be seen from Fig. 5.2, the curves relative to the cases with and without the nodal modulation are very close, highlighting the fact that its contribution is negligible both in terms of the global equilibrium configuration and of infilling velocity of the basin (Townend et al., 2007). More in detail, fig. 5.3 (a) shows the equilibrium configuration of the basin under examination and its characteristic dendritic channel network, while (b) highlights the increase in time-averaged equilibrium bottom depth obtained by taking into account for the nodal tide. It can be seen that, under the effect

of the nodal tide, the channels are just a few centimeters less deep, while the difference on the shoals and on the marshes is of the order of some millimeters. In fact, with negligible horizontal net fluxes, the final equilibrium configuration ($C = C_{eq}$ in Eq. 5.2) of a lagoon and, up to a point, the slow adaptation process, is expressed by Eq. 5.1 with $C_{eq} = C_{INLET} = const$. In these conditions the value of $h(x, y)$ is affected by the nodal tide only by an increase of q_{tc} of about 4% active only in the channels. Although

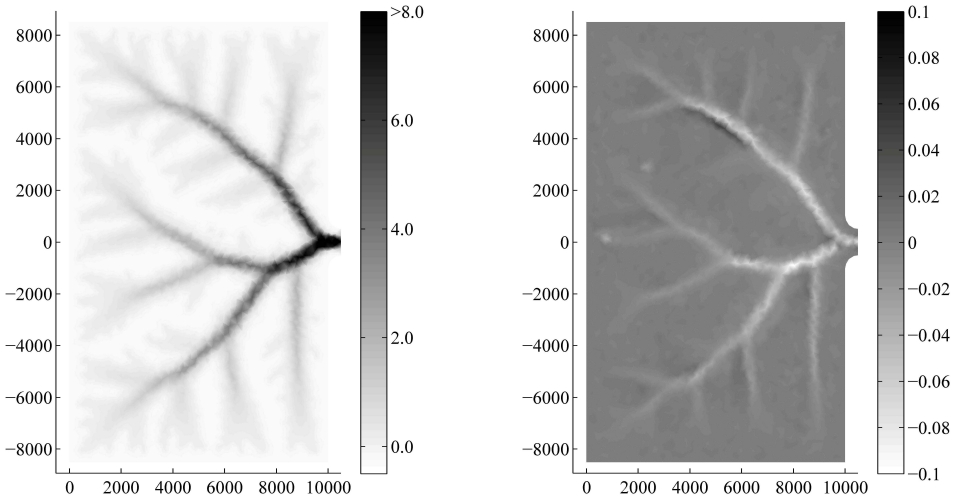

(a) Equilibrium depth, no nodal tide (m)

(b) Increase in time-averaged depth due to nodal tide (m)

Figure 5.3: Equilibrium conditions: effect of the nodal tide

the nodal contribution can eventually be considered not to have a significant influence on the long-term evolution and equilibrium conditions of the basin, at a shorter (so to say, *sub-nodal*) time scale, non-negligible morphodynamic processes can locally take place. In fact, the channel depth at the inlet is subject to an oscillation with 0.5 m amplitude (Fig. 5.4, a), corresponding to a relative oscillation of 6-17%, much larger than the nodal value of 4%. The absolute oscillation progressively decreases along the channel network reaching smaller values at the end of the channel branches and on the shoals. Nevertheless, shoals and salt marshes are the morphological features in which

the relative oscillation amplitude of the bottom depth is greater, as shown in Fig. 5.4, b). Coming to the phase lag in the morphological response of the different sections of the basin, it has been found (Fig. 5.4, c) that the bottom depth response, referred to the mean sea level, is very prompt and nearly synchronous along the channel network, with a phase lag of 0 to 2 years. This value is more etherogeneous, and generally ramarkably greater, on the shallow zones. In particular, a 9-years phase difference between the channels and the neighbouring shoals suggests the presence of an alternate sediment flux between these sections of the lagoon.

The sediment fluxes through the inlet oscillate with a phase lag of 6.4 years with respect to the nodal modulation and with an amplitude of 2.05E+5 m^3/yr, with a net average inflow due sea level rise (Bonaldo and Di Silvio, 2011a). Differently from what seen for the bottom depth, suspended sediment concentration fluctuates (Fig. 5.5) with maximum amplitude (2 ppm, namely 10 % of the concentration at the boundary) in the middle of the basin, while this value is zero on the inlet, where the concentration is prescribed, and is small although non-zero in the peripheral zones of the basin where the transport processes are less active. The phase pattern shows a significant lag along the channel nework, appearantly decreasing on the shoals: in fact, it seems more likely that this result is due to a response time exceeding the nodal period on the peripheral zones of the lagoon.

A simple application of the one-element version of ASMITA (Kragtwijk et al., 2004) shows that the expected phase lag for the system as a whole is about 11.4 years, qualitatively between the very small value in the channels and the higher value of the shoals.

5.3.2 Effect of the forcing factors

The results of the simulations summarized in Tab. 5.1 were compared mainly in terms of their global properties. Nevertheless, some interesting evidences have been also drawn

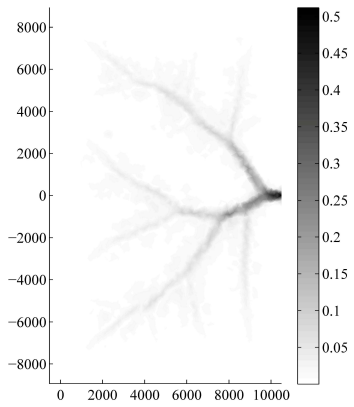

(a) Bottom depth oscillation absolute amplitude (m)

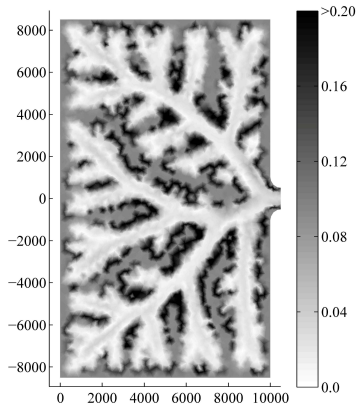

(b) Bottom depth oscillation relative amplitude (-)

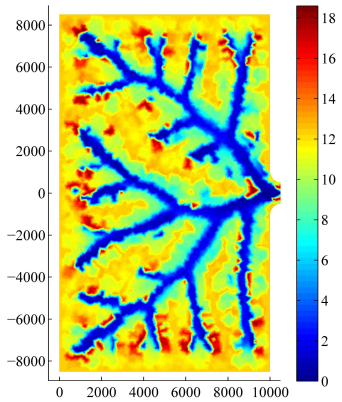

(c) Bottom depth oscillation phase (y)

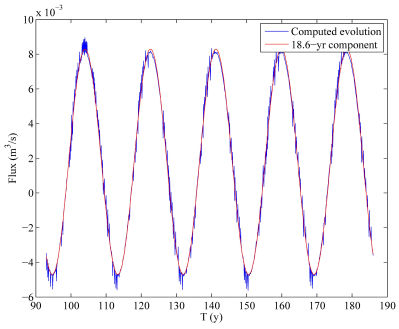

(d) Sediment fluxes through the inlet

Figure 5.4: Bathymetric oscillations and sediment fluxes due to nodal tide

by considering the spatial distribution of some quantities. Some qualitative behaviours reported in Subs. 5.3.1 have been confirmed confirmed in all the considered scenarios. This is the case of the fast response of the absolute channel depth decaying in amplitude from the mouth towards the interior of the basin, and a relative oscillation which can be greater than the 4% value of the nodal perturbation, especially on the shoals. The con-

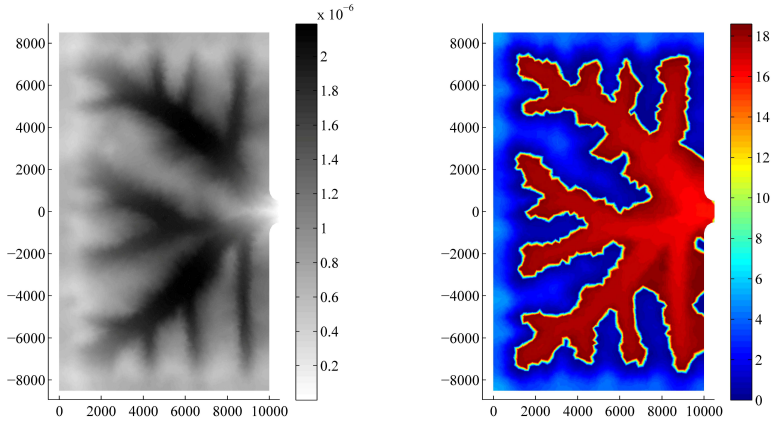

(a) Suspended concentration oscillation amplitude (-)

(b) Suspended concentration oscillation phase (y)

Figure 5.5: Suspended concentration oscillations due to nodal tide

centration, on the other hand, exhibits an oscillation whose amplitude increases moving from the inlet (with a slightly preferential direction along the channel network) until reaching a maximum, generally of the order of 10% the concentration at the inlet, and then decreasing again.

Concerning the global properties, they have been reconstructed by using just their nodal component, and described in the general form:

$$Y = \overline{Y} + A \sin\left(2\pi \frac{t}{\tau} + \Phi\right) \tag{5.4}$$

where Y is the considered quantity, $\overline{Y}$ its time-averagd value, A the oscillation amplitude, t and τ respectively the time and the nodal period (namely, 18.6 years), and Φ the phase lag with respect to the nodal modulation. The values of $\overline{Y}$, A and Φ for each of the properties under analysis have been resumed in Tab. 5.2.

Although influencing the morphological properties of the basin (Di Silvio et al., 2010), none of the parameters considered here to distinguish the eleven scenarios (with the obvious exception, but only in absolute terms, of the mean tidal range, see Sim. 7) appears to affect the way the nodal modulation influences the very same global prop-

	Sed. fluxes (m^3/s)			**Veg. cover (%)**		
Sim.	$\overline{Y}$	A (m^3/s)	Φ (y)	$\overline{Y}$	A (%)	Φ (y)
1	1.79E-03	6.49E-03	6.40E+00	3.63E+01	3.00E-01	1.21E+01
2	3.45E-03	6.25E-03	6.30E+00	3.61E+01	3.10E-01	1.12E+01
3	5.05E-05	6.70E-03	6.50E+00	3.64E+01	3.00E-01	1.06E+01
4	-9.40E-04	6.20E-03	6.60E+00	0.00E+00	0.00E+00	0.00E+00
5	1.78E-03	5.92E-03	6.50E+00	0.00E+00	0.00E+00	0.00E+00
6	-1.00E-05	6.40E-03	6.60E+00	0.00E+00	0.00E+00	0.00E+00
7	1.78E-03	1.30E-02	6.30E+00	2.87E+01	1.75E-01	1.83E+01
8	2.03E-03	6.19E-03	6.30E+00	4.40E+01	3.00E-01	1.03E+01
9	4.50E-04	1.34E-03	6.00E+00	5.20E+01	3.00E-01	1.28E+01
10	1.11E-04	2.70E-04	5.30E+0	6.43E+01	4.70E-01	9.80E+00
11	1.20E-03	8.40E-03	6.50E+0	3.33E+01	2.30E-01	1.21E+00
	Water Volume (m^3)			**Mean Depth (m)**		
Sim.	$\overline{Y}$	A (m^3)	Φ (yr)	$\overline{Y}$	A (m)	Φ (y)
1	1.05E+08	2.90E+06	3.00E-01	2.66E-01	4.00E-03	1.70E+00
2	1.07E+08	2.88E+06	3.00E-01	2.80E-01	3.32E-03	1.80E+00
3	1.03E+08	2.92E+06	4.00E-01	2.50E-01	3.70E-03	1.80E+00
4	1.40E+08	3.03E+06	4.00E-01	4.70E-01	4.20E-03	1.50E+00
5	1.47E+08	2.86E+06	3.00E-01	5.10E-01	3.24E-03	1.80E+00
6	1.42E+08	2.70E+06	4.00E-01	4.80E-01	3.36E-03	1.90E+00
7	1.93E+08	5.82E+06	3.00E-01	4.30E-01	7.07E-03	1.70E+00
8	9.05E+07	2.91E+06	3.00E-01	1.80E-01	3.50E-03	1.70E+00
9	1.69E+07	7.11E+05	2.00E-01	4.60E-02	2.91E-03	1.30E+00
10	2.80E+06	1.74E+05	1.00E-01	-8.70E-02	2.38E-03	6.00E-01
11	1.66E+08	3.03E+06	4.00E-01	6.22E-01	4.37E-03	1.90E+00

Table 5.2: Global effects of nodal tide on various quantities for the examined scenarios ($\overline{Y}$: time-averaged value; A: oscillation amplitude; Φ: phase lag)

erties. Even the planimetric configuration of the basin (which controls the relative importance of channels and shoals) does not seem to play a significant role on the effects

exerted by the nodal perturbation on the morphological behaviour (Sim. 11), although this result must be considered with some attention. In fact, it must be noted that for a long and narrow estuary the wind stirring coefficient is propbably excessive while the hypothesis of short basin (namely of instantaneous propagation of the tidal wave) is not valid anymore. As already said, however, the aim was not to represent a real situation but rather to assess the role of the geometric constraint.

5.4 Conclusions

The effect of the nodal tide modulation on the morphological behaviour of a microtidal short lagoon has been investigated under different conditions. It has been shown that the nodal contribution can be neglected in very long evolutions, since the time-averaged effect over the nodal period, although non-zero, is small and spatially concentrated. By contrast, on a shorter (sub-nodal) term, relevant oscillating sediment fluxes take place both at the inlet, between the sea and the lagoon, and between channels and shoals. These give rise to temporary modifications of the morphology of the lagoonal sections, and especially of the shoals, which may explain some unespectedly remarkable changes of lagoon morphology. While the response to the nodal tide in the channel network is nearly symultaneous, (in agreement with other type of perturbations (Bonaldo and Di Silvio, 2011b)) the response time of the shoals is more heterogeneous, suggesting the presence of a complex sediment flux pattern which should possibly be better investigated.

The same behaviour for the spatial distribution of oscillation amplitude and phase of two relevant quantities (suspended concentration and bottom depth) was found for largely different conditions of wind effect, sea level rise, grainsize and system geometry. In some configurations, the response time of some peripheral sectors of the system exceeds the nodal period (negative lag), but this does not seem to have any impact on the

overall evolution of the system.

The salt marshes appear to be minorly affected by the nodal oscillation of tidal range, possibly because of their intrinsic resilience due to the sediment trapping and bottom strenghtening of the alophile vegetation cover.

Chapter 6

Final Remarks

6.1 Applications and limits of the *Intertidal Model*

The Intertidal Model presented in this Thesis aims to provide some generalizations to the existing long-term morphodynamic models for tidal environments.

The *intertidal dispersion* concept allows a simple and computationally cheap representation the net sediment transport. This is described in terms of *transport concentration*, which is an additive quantity, thus relatively easy to treat particularly in presence of different sediment sources. The definition of an *equilibrium concentration* as a sum of the effect of several entrainment factors permits to disaggregate the single contributions and investigate the response to different external contraints. A criterion for the experimental calibration of the stirring coefficients has also been proposed.

An important novelty with respect to some previous formulations based on the same concepts (Di Silvio and Padovan, 1998) is that hydrodynamics is separately computed by a dedicated, though simplified, sub-model. This implies that it is possible to reproduce the mutual interactions between water flow and morphodynamic processes and, moreover, there is no need for any *a priori* definition of the morphological features of the lagoon.

It is now worth to point out that long-term equilibrium can be defined in two different ways. A definition based on nil vertical and horizontal net fluxes of sediments requires that the concentration is spatially uniform and the bathymetry is constant in time. This "static" condition can only be achieved in absence of sediment sources or sinks, and appears rather unrealistic. A less restrictive definition is based on a "dynamic" condition in which the bathymetry is again constant in time, but as an effect of a stable configuration of balanced, and non zero, horizontal and vertical fluxes. This is the case, for example, of a basin infilling under the effect of sea level rise or soil compaction: these factors establish a dynamic equilibrium condition characterised by a concentration gradient between the inlet and inner boundary of the basin, related to an inward net sediment flux.
The model can be applied to the investigation of long-term morphodynamic processes in short tidal environments: this restriction is due to the assumptions made in the flow submodel, but can be overcome by increasing the complexity of the hydrodynamic description. Equilibrium (either "static" or "dynamic") conditions can also be studied under several combinations of the forcing factors.
The criterion defined for estimating the stirring coefficients for sea waves at the inlet allows to estimate the boundary conditions for the system also in absence of an explicit representation of the littoral dynamics. Nevertheless, as will be explained further on, the introduction of a conceptualization of the coastal processes could be a most relevant improvement of the model.
Although the phenomena are treated with a two dimensional approach, and so are the results, the model is mainly oriented to the computation of the global properties of the system (e.g. average bottom depth, hypsometry, surface areas of the morphological features, etc.). In fact, the planimetric structure of some results (channel network geometry, meanders, etc.) must be interpreted very carefully, as their realism may be significantly invalidated by the absence of a detailed description of some processes and by the mesh resolution. Nevertheless, while the mesh size has been found to be a key parameter in

defining the structure of the resulting channel network, some sensitivity analyses shown that it does not affect the global properties.
The results presented in Chapters 3 and 4 show a quite anomalous granulometric selection on the salt marshes, which appear generally coarser than the neighbouring shoals. As it has been discussed, this result is consistent with the model formulation, but is in contrast with some field observations. This shortcoming can be possibly explained with the absence of cohesive sediments, since the introduction of a different entrainment and deposition behaviour could reasonably provide a more realistic result, especially in low-energy environments such as salt marshes and shoals.

6.2 River modelling at basin scale

As it will be shown in Sec. 6.3, the Intertidal Model is likely to be generalized in a regional-scale model in which the fluvial, estuarine and coastal systems mutually interact in shaping the landscape. In this framework, the rivers provide not only the boundary conditions, but they represent a part of the system considered as a whole. For this reason it appears sensible to briefly summarize a simplified long-term morphodynamic model formulated by Di Silvio and Peviani (1989) and recently improved by Ronco et al. (2009), and the novelties introduced during the early stage of the Candidate's Ph.D. activity (Di Silvio et al., 2009).
River modelling should take into account the mutual interactions of three factors: hydrodynamics, morphodynamics and vegetation growth. In principle, all these factors have 3-D or, at least, 2-D features. On the other hand, in order to deal with the problem at basin scale (up to hundreds or thousands kilometres) and at the time-scale of decades or centuries, a computationally cheap 1-D model which describes water and sediment movement along the river (Di Silvio and Peviani, 1989; Ronco et al., 2009) based on

the hypothesis of *Local Uniform Flow* (Fasolato et al., 2011), has been improved with a schematic description of the transversal evolution of river bed and riparian vegetation. The 2-D or 3-D aspects of hydrological, morphological and vegetational processes are somehow put into account by a cross-section submodel of the bare profile and its vegetation cover. The entire model, however, is in principle still one-dimensional, being the evolution of the river cross-section solely controlled by the longitudinal variations of the one-dimensional variables (waterflow, sediment transport, bottom elevation, slope and bottom composition), via simple algebraic equations or time-depending ordinary differential equations.

In particular, the transversal profile is basically controlled by the local slope and annual duration curve of waterflow and the occupancy of the cross-section by vegetation (considered for the moment as only one representative species) is controlled by the waterflow duration curve and the cross-section profile (Nones, 2012).

The model response to a relevant reduction of equivalent discharge (lowering of the waterflow duration curve) indicates, as expected, a reduction of the "effective" river width, an increase of vegetation and a contemporary deeper incision of the river main channel. The model, however, may definitely give more satisfactory results by a more accurate calibration based on detailed data of riparian vegetation, including different species, and by relaxing some restrictive hypotheses (Di Silvio et al., 2009).

6.3 Towards an integrated coastal model

This is an attempt to extend the approach used in the representation of tidal lagoons to the coastal environment, allowing to study with a unified conceptualization fluvial, estuarine and littoral systems and their interactions. The endeavour is mainly the analysis of the processes acting in the genesis and evolution of the coastal landscape, but this approach can also be used for large-scale and long-term sediment budgets on littoral

regions.

The challenge is to find a description of the problem simple enough to be consistent with the model framework but containing, although with some assumptions, all the characteristic dynamics of the coastal system. The main issue is the description of the cross-shore sediment transport, which control the equilibrium beach profile, while the long-shore transport can be easily described by using some well-known empirical equations. Several conceptualizations, with different degrees of simplification, have been considered and are briefly explained below.

The simplest idea was to maintain the "ellipticity" of the problem, i.e. to represent the cross-shore transport by means of dispersive terms alone. This implies that, in equilibrium, the concentration is supposed to be uniform: which is quite a strong assumption and definitely contrary to experimental evidence. Therefore some other transport mechanisms should be hypothesized which compensate the dispersive flux. Moreover an equilibrium concentration needs to be defined as a function of bottom depth and distance from the shore (or slope, but in this case the numerical solution becomes vulnerable to instability issues) in such a way to provide a bottom profile as defined by Dean (1977):

$$h(s) = As^{2/3} \tag{6.1}$$

where A is a coefficient containing the information regarding the sediments and s is the cross-shore coordinate.

Thus it was decided to include a further transport term (which will be defined later on) in the system: this, coupled with the dispersive one, allows to have a steady non-uniform equilibrium concentration profile also in absence of net fluxes. To do that, a deeper insight in the physical transport processes originated by waves is necessary in order to decide what is worth to be explicitly taken into account.

Cross-shore sediment dynamics are characterized by both bed load and suspended load transport phenomena, and the main processes pointed out are the following:

- Time-averaged bottom shear stress due to non-linear waves;
- Streaming currents acting on the boundary layer;
- Gravity;
- Undertow;
- Wind effects;

Since the main model works in terms of total load without any distinction between bed and suspended load (this is due to the vertical averaging operation), the separate treatment of all the processes mentioned above would require a few assumptions (with some degree of arbitrariness) in order to properly quantify the net contribution of each term. Moreover, such a detailed description introduces an unnecessary complexity in the model, hence a further simplification is required.

By assuming that the main dispersive effect is provided by the wave orbital velocity, one can either define a "behaviour-oriented" *pseudo-advection* such to provide, in equilibrium, a "Dean-type" profile, or find out one or two dominant advective processes for the cross-shore sediment transport and follow a process-based approach. The concept of *pseudo-advection* is meant here as a net sediment transport along a dominant direction in absence of a corresponding net transport of water, as it may occur for asymmetric alternate waterflow produced by waves or currents (this is the case, for example, of the net loss of sediments from an ebb-dominated basin).

It should also be decided whether to consider or not the different behaviour of waves within the breaking zone. In fact, in this part of the domain the incoming waves dissipate the major part of their energy and drastically decrease their height: for this reason, the equilibrium concentration profile generated by sea waves (Chap.2) should have, strictly speaking, a maximum in proximity of the breaking zone and then decrease towards the shore. The maintenance of such a profile, though this conceptualization is more precise

and directly related to the local wave, requires a convergence of the advective flow field towards the breakers' line. In synthesis, two choices must be made for the description of the problem: the first one is between behaviour-oriented and process-based model, and the other one is between monotonic and non-monotonic equilibrium concentration profile. For a preliminary test a behaviour-oriented monotonic representation seems the appropriate choice: this is the simplest formulation and it is consistent with the degree of detail of the model.

It is easy to see that an estimate of the wave field cannot be disregarded, hence some wave models were considered and compared. In particular, we were looking for a way to represent shoaling, refraction and, if possible, diffraction of a monochromatic "Morphological wave" (Chesher and Miles, 1992).

First of all we considered a back-tracking ray based model (Teluram), which is very simple but, being a point model, does not comply with our requirements. Then the choice was basically between a model based on the solution of the Mild Slope Equation (in particular RefDif was considered, solving the parabolic approximation of the MSE) and a spectral wave model, based on the solution of an Energy Balance Equation (SWAN). Both of them can reproduce shoaling, refraction and diffraction (although SWAN represents diffraction in a simplified way, which restricts the range of possible applications, but in a way that does not affect our work), but SWAN seems to some extent more versatile, being able to provide some more information which can prove to be useful: this is the reason why it was eventually chosen.

The sediment transport equation for the modified model can then be written (for sake of simplicity in the unigranular formulation) as follows:

$$\nabla q_s + \nabla UhC - \nabla \mathbf{D} h \nabla C = E; \tag{6.2}$$

where q_s is the pseudo-advective solid transport.

Preliminary feasibility tests were carried out, with encouraging results, in a one-dimensional ideal beach profile in which the pseudo-advective term was defined in such a way to pro-

vide, in equilibrium, a stable “Dean” profile.

In this final Chapter I endeavoured my efforts in summarizing and gathering some tools for long-term morphodynamic at regional or, so to say, landscape scale. A model for the tidal environments, though still susceptible of some improvements, has been presented and discussed throughout this Thesis; a fluvial model was briefly introduced in Sec. 6.2 and the conceptual framework for the introduction of a coastal module in the Intertidal Model was sketched in the present Section. The goal now is to merge all these instruments together in a unified approach.

Bibliography

Armanini, A., and Di Silvio, G., 1988. A one-dimensional model for the transport of a sediment mixture in non-equilibrium conditions. Journal of Hydraulic Research 26 (3), 275-292.

ASCE Manual 54, *Sedimentation Engineering*, 1975. Vanoni, V.A. (Ed.), Reston, Virginia.

Barillari, A., 1977-78. Prime notizie sulla distribuzione dei sedimenti superficiali nel bacino centrale della Laguna di Venezia (in Italian). Atti Ist. Veneto di SS.LL.AA., 136, Venice, Italy.

Barillari, A., 1980-81. Distribuzione dei sedimenti superficiali nel bacino meridionale della Laguna di Venezia (in Italian). Atti Ist. Veneto di SS.LL.AA., 139, Venice, Italy.

Blondeaux, P., De Bernardinis, B., Seminara, G., 1982. Correnti di marea in prossimit di imboccature e loro influenza sul ricambio lagunare (in Italian). Atti del XVIII Convegno di Idraulica e Costruzioni Idrauliche, Bologna, Italy, 21-23 Sept.

Bonaldo, D., Dall'Angelo, C., Di Silvio, G., 2010. Trasporto Mareale di Sedimenti a Granulometria non Uniforme (in Italian). XXXII Convegno Nazionale di Idraulica e Costruzioni Idrauliche, 14-17 Sept., Palermo, Italy.

Bonaldo, D., and Di Silvio, G., 2011. Morphodynamic modelling of a tidal basin in presence of graded sediments. Submitted to *Continental Shelf Research*.

Bonaldo, D., and Di Silvio, G., 2011. Historical evolution of a micro-tidal lagoon simulated by a 2-D schematic model. Submitted to *Geomorphology*.

Bonaldo, D., and Di Silvio, G., 2011. Morphological consequences of the nodal modulation on a tidal lagoon. Submitted to *Marine Geology*.

Brambati, A., Catani, G., Marocco, R., 1977. Indagini sedimentologiche sulla spiaggia sottomarina dell'Adriatico settentrionale tra i fiumi Brenta e Tagliamento (in Italian). Boll. Soc. Geol. It. 96, 69-86.

Brancolini, G., Tosi, L., Baradello, L., Donda, F., Zecchin, M., 2006. The subsoil architecture of the lagoon and gulf of Venice (Italy) by very high resolution seismic surveys in shallows. In Scientific Research and Safeguard of Venice, Research Programme 2004-2006, Vol. VI, 2006 results, 517-561.

Carniello, L., Defina, A., D'Alpaos, L., 2009. Morphological evolution of the Venice lagoon: Evidence from the past and trend for the future. Journal of Geophysical Research, 114.

Camuffo, D. 1993. Analysis of the sea surges at Venice from A.D. 782 to 1990. Theoretical and Applied Climatology, 47(1), 1-14.

Chesher, T. J., and Miles, G. V., 1992. The concept of a single representative wave for use in numerical models of long term sediment transport predictions. in Proceedings of the Second International Conference on Hydraulic and Environmental Modelling of Coastal, Estuarine and River Waters, Volume 1, edited by Falconer, Chandler-White and Liu, pp. 371-380, Cambridge, UK.

D'Alpaos, L., 2010a. L'evoluzione morfologica della Laguna di Venezia attraverso la lettura di alcune mappe storiche e delle sue carte idrografiche (in Italian). Ed. Comune di Venezia, Istituzione Centro Previsioni e Segnalazioni Maree, Special Law for Venice, Venice, Italy.

D'Alpaos, L., 2010b. Fatti e misfatti di idraulica lagunare. La laguna di Venezia dalla diversione dei fiumi alle nuove opere delle bocche di porto (in Italian). Ed. Istituto Veneto di Scienze, Lettere ed Arti, Venice, Italy.

Dal Monte, L., and Di Silvio, G., 2003. Ratio between channel cross-section and tidal prism in short lagoons: validity and limits of the "Law of Jarrett". 3rd IAHR Symposium on River, Coastal and Estuarine Morphodynamics, 1-5 Sept., Barcelona, Spain.

Dal Monte, L., and Di Silvio, G., 2004. Sediment concentration in tidal lagoons. A contribution to long-term morphological modelling. Journal of Marine Systems 51, 243-255.

De Vriend, H. J., 1996. Mathematical modelling of meso-tidal barrier island coast. Part I: empirical and semi-empirical models. Advances in Coastal and Ocean Engineering 2, 115149.

Dean, R. G., 1977. Equilibrium beach profiles: U.S. Atlantic and Gulf coasts, Ocean Engineering Report No. 12, Newark, Delaware.

Di Silvio, G., and Armanini, A., 1981. Influence of the Upstream Boundary Conditions of the Erosion-Deposition Processes in Open Channles. XIX IAHR Congress, Paper 22, sub A (a), New Delhi, India.

Di Silvio, G., and Fiorillo, G., The experience of Venice, Transport Models for Inland and Coastal Waters, ed. Fisher, Academic Press, 1981,112.

Di Silvio, G., Modelling the morphological evolution of tidal lagoons and their equilibrium configurations. Proceedings of the XXIII IAHR Congress, 1989 Ottawa, Canada, C169-C175.

Di Silvio, G. and Peviani, M. A., 1989. Modelling short-and long-term evolution of

mountain rivers: an application to the torrent Mallero (Italy). Published at: International Workshop on fluvial hydraulics of mountain regions. Trent, Italy

Di Silvio, G., and Teatini, P., 1992. Conterminazione Lagunare, Istituto Veneto di Scienze, Lettere ed Arti, VII, Venice, Italy.

Di Silvio, G., and Padovan A., 1998. Interaction between marshes, channels and shoals in a tidal lagoon investigated by a 2-D morphological model. 3rd Int. Conf. on Hydroscience and Engineering. Cottbus, Berlin, Germany, 3, CD-ROM.

Di Silvio, G., Barusolo, G., Sutto, L., 2001. Competing driving factors in estuarine landscape. 2nd IAHR Symposium on River, Coastal and Estuarine Morphodynamics, Obihiro (Japan), 10-14 Sept.

Di Silvio, G., Dal Monte, L., 2003. Ratio between channel cross-section and tidal prism in short lagoons: validity and limits of the Law of Jarrett. In: Final Proceedings of the Third IAHR Symposium on River, Coastal and Estuarine Morphodynamics, Barcelona, Spain, vol. 1, pp. 52533.

Di Silvio, G., Bonaldo, D., Nones, M., 2009. Morphological and vegetational response to hydrological changes in rivers. 33rd IAHR Congress, Vancouver, British Columbia, Canada, August 9-14, 2009.

Di Silvio, G., Dall'Angelo, C., Bonaldo, D., and Fasolato, G., 2010. Long-term model of planimetric and bathymetric evolution of a tidal lagoon. Continental Shelf Research 30, 894-903.

Dronkers, J., 1978. Longitudinal dispersion in shallow well-mixed estuaries. Coast. Eng. Conf. 3, 169.

Dronkers, J., 1986. Tidal asymmetry and estuarine morphology. Netherlands Journal of Sea Research 20 (2/3), 117131.

Fasolato, G., Ronco, P., Langendoen, E. J., Di Silvio, G., 2011. Validity of Uniform Flow Hypothesis in One-Dimensional Morphodynamic Models. J. Hydraul. Eng. 137, 183.

Favero, V., Serandrei Barbero, R., 1980. Origine ed evoluzione della laguna di Venezia - bacino meridionale (in Italian). Lavori della Societ Veneta di Scienze Naturali, Vol. 5, 49-71. Venice (Italy), January 1st 1980.

Ferrarin, C., Cucco, A., Umgiesser, G., Bellafiore, D., Amos, C. L., 2010. Modelling fluxes of water and sediment between Venice Lagoon and the sea. Continental Shelf Research 30, 904-914.

Fontana, A., Mozzi, P., Bondesan, A., 2008. Alluvial megafans in the Venetian-Friulian Plain (north-eastern Italy): Evidence of sedimentary and erosive phases during Late Pleistocene and Holocene. Quaternary International 189, 71-90.

Gratiot, N., Anthony, E.J., Gardel, A., Gaucherel, C., Proisy, C., Wells, J.T., 2008. Significant contribution of the 18.6 year tidal cycle to regional coastal changes. Nature Geosci, 1(3), 169-172.

Jeuken, M.C.J.L., Wang, Z.B., Keiller, D., Townend, I., Liek, G.A.,2008. Morphoological response of estuaries to nodal tide variation. International Conference in Estuaries and Coasts, November 9-11, 2003, Hangzhou, China.

Karunarathna, H., Reeve, D., Spivack, M., 2008. Long-term morphodynamic evolution of estuaries: an inverse problem. Estuarine Coastal and Shelf Science, 77, 385-395.

Kragtwijk, N.G., Zitman, T.J., Stive, M.J.F., Wang, Z.B., 2004. Morphological response of tidal basins to human interventions. Coastal Engineering 51, 207-221.

Lanzoni, S., and Seminara, G., 2002. Long-term evolution and morphodynamic equilibrium of tidal channels. J. Geophys. Res. 107.

Magistrato alle Acque di Venezia and Corila, 2006. Unpublished Report.

Marani, M., Lanzoni, S., Belluco, E., DAlpaos, A., Defina, A., Rinaldo, A., 2003. On the drainage density of tidal networks. Water Resources Research 39 (2), 105113.

Molinaroli, E., Guerzoni, S., Sarretta, A., Cucco, A., Umgiesser,. G., 2007. Links between hydrology and sedimentology in the Lagoon of Venice, Italy. Journal of Marine Systems 68 (3-4), 303-317.

Nones, M., 2012. Aspects of riverine hydro-morpho-biodynamics at watershed scale. Ph. D. Thesis, Universitá degli Studi di Padova, Padua, Italy.

O' Brien, M.P., 1931. Estuary tidal prism related to entrance areas. Civil Engineering, 1(8), 738-739.

Okubo, A., 1973. Effect of shoreline irregularities on streamwise dispersion in estuaries and other embayments. Netherlands Journal of Sea Research 6 (1-2), 213-224.

Oost, A.P., de Haas, H., Ijnsen, F., van den Boogert, J.M., de Boer, P.L., 1993. The 18.6 yr nodal cycle and its impact on tidal sedimentation. Sedimentary Geology 87, 1-11.

Pugh, D.T., 1996. Tides,Surges and Mean Sea-Level (reprinted with corrections). John Wiley & Sons Ltd., Chichester, UK, 486 pp.

Ray, R.D., 2006. Secular changes of the M2 tide in the Gulf of Maine. Continental Shelf Research 26, 422-427.

Rinaldo, A., Fagherazzi, S., Lanzoni, S., Marani, M., Dietrich, W.E., 1999. Tidal networks: 3 - landscape-forming discharge and studies in empirical geomorphic relationship. Water Resources Research 35 (12), 39193929.

Ronco, P., Fasolato, G., Di Silvio, G., 2009. Modelling evolution of bed profile and grain size distribution in unsurveyed rivers. International Journal of Sediment Research, Volume 24, Issue 2, June 2009, Pages 127-144

Sarretta, A., Pillon, S., Molinaroli, E., Guerzoni, S., Fontolan, G., 2010. Sediment budget in the Lagoon of Venice, Italy. Continental Shelf Research 30(8), 934-949.

Serandrei Barbero, R., Lezziero, A., Albani, A., Zoppi, U., 2001. Depositi tardo-pleistocenici ed olocenici nel sottosuolo veneziano: paleoambienti e cronologia (in Italian). Il Quaternario 14(1), 9-22.

Schijf and Schönfeld, J.C., 1953. Theoretical considerations on the motion of salt and fresh water. Proc. 5th. Cong. Intl. Assoc. for Hydr. Res, Minnesota, 321-333.

Shaw, A.G.P., and Tsimplis, M.N.,2010. The 18.6 yr nodal modulation in the tides of Southern European coasts. Continental Shelf Research 30, 138-151.

Stive, M.J.F., Wang, Z.B., Capobianco, M., Ruol, P., Bujsman, M.C., 1998. Morphodynamics of a tidal lagoon and adjacent coast. In: Dronkers, J., Sheffers, M.B.A.M. (Eds.), Physics of Estuaries and Coastal Seas. Balkema, Rotterdam, 397-407.

Tambroni, N., Seminara, G., 2006. Are inlets responsible for the morphological degradation of Venice Lagoon? J. Geophys. Res. 111.

Tonetto, C., 2009. Evaluation of the intertidal dispersion coefficient for a morphodynamic model of a tidal lagoon. Master Thesis, Universitá degli Studi di Padova, Padua, Italy.

Townend, I., Amos, C., 2008. Estuary and inlet morphodynamics and evolution. In: Final Proceedings of the IX Congress, Littoral, Venice, T8, CD ROM.

Townend, I.H., and Whitehead, P.A., 2003. A preliminary net sediment budget for the Humber Estuary. The Science of the Total Environment, 314-316, 755-767.

Townend, I.H., Wang, Z.B., Rees, J.G., 2007. Millennial to annual volume changes in the Humber Estuary. Proceedings of the Royal Society 463, 837-854.

Townend, I., 2010. An exploration of equilibrium in Venice Lagoon using an idealised form model. Continental Shelf Research 30 (8), 984-999.

Townend, I., 2011. Predicting the morphology of UK estuaries using a 3D form model. In: River, Coastal and Estuarine Morphodynamics (RCEM 2011), 6-8 September 2011, Beijing, China. (2011).

Van Ledden, M., Van Kesteren, W.G.M., Winterwerp, J.C., 2004a. A conceptual framework for the erosion behaviour of sandmud mixtures. Continental Shelf Research 24, 1-11.

Van Ledden, M., Wang, Z.B., Winterwerp, H., De Vriend, H., 2004b. Sand-mud morphodynamics in a short tidal basin. Ocean Dynamics 54, 385-391.

Wang, Z.B., Karssen, B., Fokkink, R.J., Langerak, A., 1998. A dynamic-empirical model for estuarine morphology. In: Dronkers, J., Scheffers, M.B.A.M. (Eds.), Physics of Estuaries and Coastal Seas. Balkema, Rotterdam, pp. 279286.

Wang, Z.B., Jeuken, M.C.J.L., Gerritsen, H., de Vriend, H.J., Kornman, B.A., 2002. Morphology and asymmetry of the vertical tide in the Westerschelde estuary. Continental Shelf Research 22, 25992609.

Wang, Z.B., de Vriend, H.J., Stive, M.J.F., Townend., I.H., 2007. On the parameter setting of semi-empirical long-term morphological models for estuaries and tidal lagoons. In: River, Coastal and Estuarine Morphodynamics, Taylor & Francis, London, pp. 103-111.

Woodworth, P.L., 2010. A survey of recent changes in the main components of the ocean tide. Continental Shelf Research 30, 1680-1691.

Yndestad, H., Turrell, W.R., Ozhigin, V., 2008. Lunar nodal tide effects on variability of sea level, temperature, and salinity in the Faroe-Shetland Channel and the Barents Sea. Deep-Sea Research I 55, 1201-1217.

Yndestad, H., 2009. The influence of long tides on ecosystem dynamics in the Barents Sea. Deep-Sea Research II 56, 2108-2116.

Zendrini, B., 1811. Memorie storiche dello stato antico e moderno delle lagune di Venezia. Tomo I e II (in Italian), 1811. Tip. del Seminario, Padova.